Feature Extraction Method based on Various Scanning Techniques in Iris Recognition System

Dissertation submitted towards the partial fulfillment of the requirement for the award of the degree of

Master of Engineering

in

Wireless Communication

Submitted by:

Kanwarpreet Kaur

Roll No: 801363017

Under the guidance of:

Dr. Kulbir Singh

Associate Professor, ECED

ELECTRONICS AND COMMUNICATION ENGINEERING DEPARTMENT

THAPAR UNIVERSITY

PATIALA – 147004 (PUNJAB)

JULY 2015

DECLARATION

I, Kanwarpreet Kaur, hereby certify that the work which is being presented in this thesis entitled **"Feature Extraction Method Based on Various Scanning Techniques in Iris Recognition System"** by me in partial fulfillment of the requirements for the award of degree of Master of Engineering in Wireless Communication from Thapar University, Patiala, is an authentic record of my own work carried under the supervision of **Dr. Kulbir Singh** (Associate Professor), **ECED.**

The matter presented in this thesis has not been submitted in any University/Institute for the award of Master of Engineering.

Date: 7 July 2015

Kanwarpreet Kaur
Roll No. 801363017

It is certified that the above statement made by the student is correct to the best of my knowledge and belief.

Date: 7 July 2015

Dr. Kulbir Singh
Associate Professor, ECED
Thapar University, Patiala

Countersigned by:

Dr. Sanjay Sharma
Professor and Head ECED
Thapar University, Patiala
Date:

Dr. S.S. Bhatia
Dean of Academic Affairs
Thapar University, Patiala
Date:

ACKNOWLEDGEMENT

Firstly, I am grateful to the God for providing me good health, wellbeing and filling me with patience that were necessary to complete my thesis work.

I would like to express my gratitude to Dr. Kulbir Singh, Associate Professor, Electronics and Communication Engineering Department, Thapar University, Patiala for his patient guidance and support throughout my work. I am truly very fortunate to have the opportunity to work with him.

I am also thankful to our Head of the Department and Professor, Dr. Sanjay Sharma and PG Coordinator Dr. Amit Kumar Kohli for providing adequate environment in carrying the work.

Also, I am extremely thankful to my parents and brother for their unceasing encouragement, support and attention. I would also like to acknowledge my friends who devoted their valuable time and helped me in all possible ways towards the successful completion of this work.

Finally, I extend my gratitude to all those persons who directly or indirectly helped me in the process and contributed towards this work.

Kanwarpreet Kaur

Roll No. 801363017

ABSTRACT

Reliable personal recognition is demand of time due to increase of terrorism and criminal offences. So, modern societies give more importance to the systems that contribute to increase of security and reliability. One of the techniques for this purpose which has proven to be very accurate and reliable is iris recognition.

Iris recognition is basically done in five steps namely; iris image acquisition, iris segmentation, iris normalization, feature extraction and feature matching. For good performance of Iris Recognition System, segmentation and normalization play an important role. Also to extract the required features from the normalized iris, feature extraction techniques are adopted. In this thesis, methods of localization and feature extraction based on various scanning techniques in iris recognition are presented.

The segmentation process in Iris Recognition System is performed based on Daugman's Integro-differential operator which is capable of localizing the iris region by assuming iris and pupil as perfect circles. Localized iris is then normalized based on Daugman's Rubbersheet model. After applying Discrete Cosine Transform on the normalized iris a method for iris feature extraction using various scanning techniques on the obtained Feature Vector coefficients is proposed. The scanning techniques used are Zigzag, Raster, and Sawtooth.

The previous work for iris feature extraction using Discrete Cosine Transform provides good results but approach of using scanning techniques in this thesis improves the accuracy percentage. Experimental results show the promising performance of Raster Type-II scanning technique with 80.30% accuracy when 100 coefficients are taken. The database used for the observations is CASIA iris database version-IV.

CONTENTS

LIST OF ABBREVATIONS AND ACRONYMS

ABIS	Automated Biometric Information System
CASIA	Chinese Academy of Sciences Institute of Automation
DCT	Discrete Cosine Transform
DFrFT	Discrete Fractional Fourier Transform
FAR	False Accept Rate
FRR	False Reject Rate
FV	Feature Vector
HD	Hamming Distance
FWT	Fast Wavelet Transform
IRS	Iris Recognition System
MFCC	Mel Frequency Cepstral Coefficient
RAM	Random Access Memory
SFC	Space Filling Curve
WED	Weighted Euclidean Distance

LIST OF FIGURES

LIST OF TABLES

CHAPTER

INTRODUCTION

1.1 INTRODUCTION

Reliable personal recognition is demand of time due to increase of terrorism and criminal offenses. So, smart and advanced societies give more importance to the systems that provides more security and reliability. Therefore, public and private operational bodies highly recommend the use of biometrics to improve traditional security systems [1]. The reason behind use of biometric area is guarding the fraudulent multiple identities [2] by taking into account an identity based on who the individual is instead on what the individual has or recollects.

Pattern recognition is a method of performing an activity based on the category of acquired raw pattern [3] and it has been received by people from a huge number of years for the sake of survival. From a few decades it is being used for individual identification (*e.g.* character, DNA and speech recognition and so forth), restorative determination, computer infection and spyware location *etc* to solve the day to-day problems. In biometrics, physiological or behavioral characteristics of individuals are acquired in order to specify their respective authentication and identification. In this way, biometrics can be seen from the pattern recognition point of view.

1.2 BIOMETRICS

Individual's automatic recognition based on their physical and behavioral characteristics is referred to as biometrics [4]. Biometrics is also referred as the branch of science and technology that measures and statistically analyses the biological data. It is usually considered as the technology for measuring and analyzing qualities of human body, for example, eye, retina and iris, finger and palm prints, voice and facial patterns, for the purpose of authentication in the field of information technology [5]. Any automatically measurable, hearty and particular physical characteristic or personal trait that can be

utilized to distinguish a person or confirm the guaranteed personality of an individual is also known as biometrics [6].

The biometrics era is said to be begun by a Portugese writer João de Barros in 14th century. For identification purpose, some of the Chinese merchants stamped children's palm and foot prints [7]. It is also believed that the ancient civilizations of China and Egypt performed recognition based on biometrics. Also, one of the biometric traits i.e. fingerprints were first used for recognition of criminals in 1891 by Juan Vucetich in Argentina [7].

The beginning of biometrics is classified into three types, named as genotypic, behavioral, randotypic [8-9]. Accordingly, there are number of biometric traits that are followed these days for the purpose of recognition such as fingerprints, face recognition, hand and finger geometry, palm-prints, iris recognition, retina recognition, vein geometry, keystroke, signature, voice or speech, cognitive biometrics.

1.3 FUNCTIONING MODES

The biometric applications for the motive of recognition, follows the procedure shown in the Figure 1.1 independent of the trait used. The procedure begins with the data acquisition where the biometric trait sample is acquired. The next step to be considered is the signature extraction in which by extracting the features from the sample, signatures are created and are referred to as biometric sample. Further a comparison is done between the acquired signatures with the available signature in the database which are commonly designated as biometric templates. If enough similarity is found between the biometric signatures, then an assumption is made that both the signatures were extracted from the same person, otherwise, both the signatures are from different persons.

The biometric recognition systems are used for various purposes but are generally part of two modes of functionality. They are either verification systems or identification systems [10].

1.3.1 VERIFICATION MODE

In verification mode of biometrics, the system verifies authenticity of a specific person who claims to be the one. Here in order to find a match, the system check for particular's biometric against a biometric profile that as of now exists in the database

connected to that individual's record [10]. Generally 1:1 matching algorithm exists in this mode.

1.3.2 IDENTIFICATION MODE

In identification mode of biometrics, the system tries to recognize the person who generated the biometric sample. After knowing the person, a comparison is made with 'N' enrolled identities or biometric samples in the database. Hence, (1:N) matching algorithm exists in this mode [10]. To identify a criminal, identification mode of biometric systems are generally opted by the government.

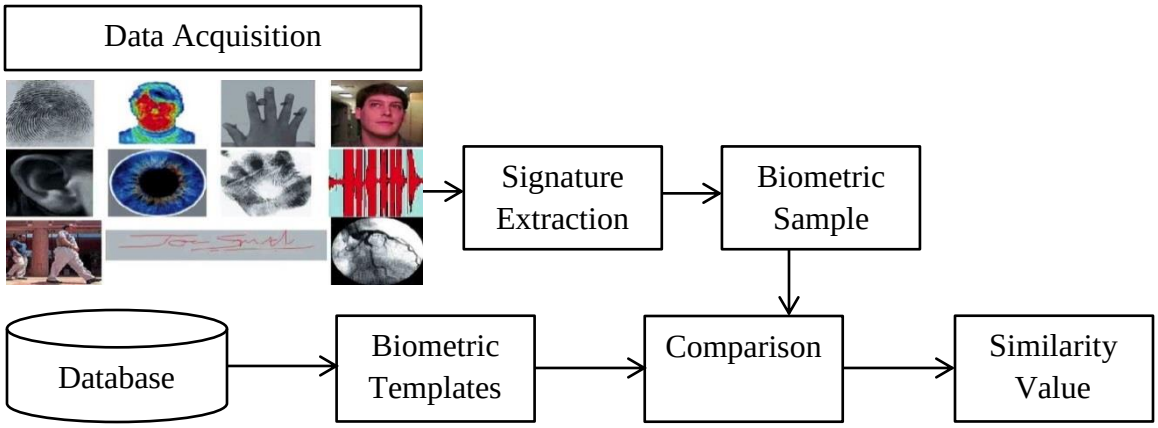

Figure 1.1: Block diagram representing stages basic stages of biometric recognition process [11-12].

1.4 BIOMETRIC TRAITS

Automatic recognition of individuals is possible using biometric systems based on their physiological and behavioral characteristics such as finger and palm prints, hand geometry, face, iris, retina, vein, signature, keystroke dynamics *etc* [13]. The most commonly used biometric traits for verification and identification purposes are briefly explained in this section. The presented traits possess high acceptability percentage by the researchers and provide many commercial applications.

1.4.1 FINGERPRINT RECOGNITION

A biometric trait, fingerprint usually appears as a pattern of complex friction ridges and valleys [7]. Fingerprint recognition based on these patterns is referred to an automatic biometric recognition method which confirms the identity of an individual when two

fingerprints are compared. On computerized systems fingerprint recognition is one of the most used biometric solutions for authentication [14].

The first fingerprint files based on Galton pattern types were introduced by Juan Vucetich in 1891 as shown in Figure 1.2 along with his signatures and he along with Galton made the world's first criminal fingerprint identification in 1892. Galton proved the uniqueness of fingerprints as 1 in 64 billion [14].

Figure 1.2: Right thumb impression and signature of Juan Vucetich [14]

1.4.2 PALMPRINT RECOGNITION

Similar to finger prints, palm prints of human hand also contain complex and unique patterns of friction ridges and valleys as shown in Figure 1.3. Being larger than finger, palm print is expected to be more distinguishable.

Generally, palm print recognition is divided into two approaches namely, feature-based and appearance-based methodologies. Feature-based methodologies fragment the palm and locate points of interest and use them whereas appearance-based approaches use the entire palm image for individual recognition [15].

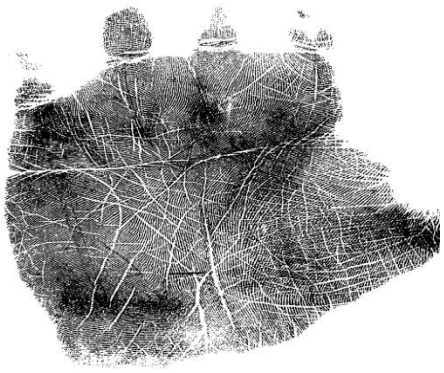

Figure 1.3: Left palm print with ridges and valleys [16]

1.4.3 FACE RECOGNITION

Human face plays a significant role in conveying people's identity and social interaction. In past several years, biometric face recognition innovation has received critical consideration utilizing the human face as a key to security. Face recognition has proved to be advantageous because of its non-contact approach as compared to finger and palm print recognitions as face images can be captured from a distance. Areas around cheekbones, upper outlines of eye sockets, location of eyes, mouth and nose are used as distinctive facial features in face recognition [17].

1.4.4 HAND AND FINGER GEOMETRY

Hand and finger geometry of a particular as shown in Figure 1.4 is considered to be unique but not as unique as other biometric traits [18]. Therefore, the geometries are used for authentication instead of identification purpose. Systems use digital camera and light to measure hand and finger geometry. The major advantages linked with this biometric system are simple imaging requirements, operatable under harsh conditions, low data storage requirements and fast processing [18].

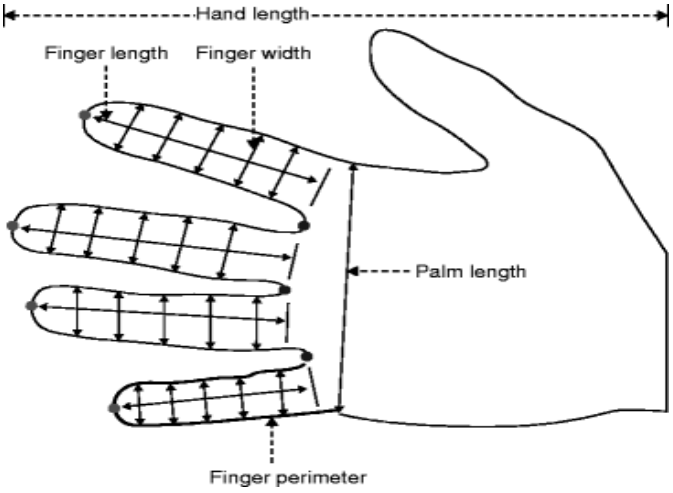

Figure 1.4: Typical hand geometry features marked on a hand contour [18]

1.4.5 RETINA RECOGNITION

Retina is a light sensitive layer of human eye which consists of neural cells and blood vessels, situated in the back segment of the eye [19] as shown in Figure 1.5 which is representing the human eye along with the locations of iris, retina *etc*. Since the structure

of the capillaries is very complex, therefore, each person's retina is unique. Even in case of identical twins, due to complex network of blood vessels in the retina, pattern doesn't match. Also, the most important advantage of considering retina recognition for identification and verification purpose is its never changing nature from birth to death [19].

1.4.6 IRIS RECOGNITION

Iris is the main inner piece of the human body which is visible from outside as shown in Figure 1.5. Its structure is extremely complex as it consists of a number of nerve fibers, muscle cells and blood vessels [19]. Extremely complex structure of iris makes it unique for every individual. Also, similar to retina and vein geometry it is a non-contact approach. The biometric system based on iris recognition is also cost effective. This technology is also capable of being used in both verification (1:1) and identification (1:N) mode of biometrics (where 'N' represents the number of templates present in the database used).

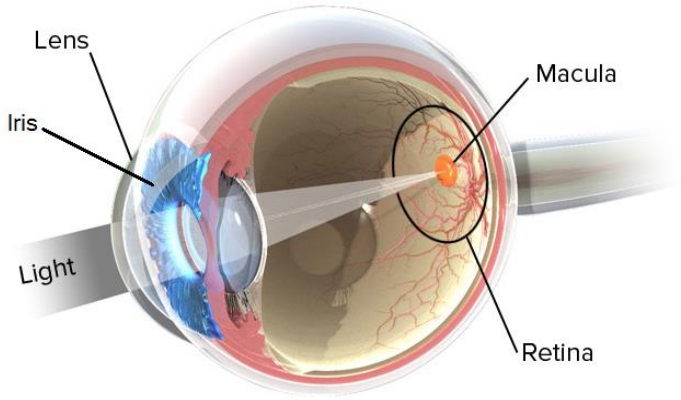

Figure 1.5: Human eye [20]

1.4.7 VEIN GEOMETRY

Vein geometry based biometric system follows contactless approach. It is believed that every person possesses unique structure and position of veins as shown in Figure 1.6 which remain unchanged from the age of ten. This is also true in case of twins. Since veins lie inside the human body, so the changes of alteration does not exist which is the main advantage of using vein geometry to fulfill the recognition motive [21].

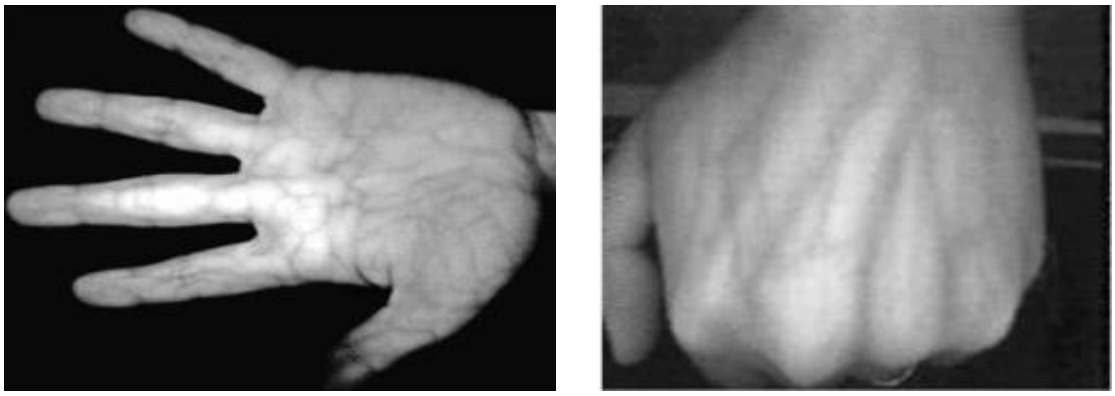

(a) Vein image on hand (b) Vein image on hand dorsum

Figure 1.6: Vein image on hand and hand dorsum [21]

1.4.8 SPEECH RECOGNITION

Voice or speech of a person is considered to be unique because pitch, shape of vocal cavities and mouth movements differs from person to person. A system working in speech recognition mode possesses the ability to receive and interpret the dictation or spoken commands. This system is used for various applications now-a-days by computer science and electrical engineering for converting speech to text after recognition or in field of identification to recognize the speaker.

1.4.9 SIGNATURE RECOGNITION

At first glance, signature recognition doesn't seem to be a good idea as there exists a number of possibilities of getting copied [18]. But biometric systems measures and examine the physical activity of signing such as speed, rhythm and pressure applied. They also make a record of sequence of forming letters, like adding dots and crosses as word finishes in a signature as shown in Figure 1.2 which has proved to be a good method in recognition field. Since signature recognition depends on physical human activity of human body while signing, hence referred to as behavioral biometric.

1.4.10 KEYSTROKE DYNAMICS

Keystroke dynamics or typing dynamics is defined as a biometric trait which measures the time for which key of the keyboard is pressed while typing a text on the computer by a person. Keystroke dynamics is a part of behavioral type biometric trait [22]. The raw

measurements used for keystroke dynamics for the authentication purpose are stay-time and flight time where stay-time is characterized as the time length of time for which a key is squeezed and flight time alluded to as the time length of time in the middle of discharging a key and squeezing the next key [22].

1.5 PARAMETER BASED COMPARISON BETWEEN THE MOST COMMON BIOMETRIC TRAITS

Jain *et al.* [23] proposed that the evaluation of biometric systems can be done on the basis of following parameters:

- Uniqueness: It is referred to the accuracy and distinctiveness of biometric attribute which measures the level of dissimilarity between individuals and system's probability of false acknowledgment.
- Universality: The biometric feature that exists in as many people as possible possesses the universal scope of the trait, such a parameter is referred as universality.
- Permeance: The quality of permanence or being unchanged throughout the life span is known as the permeance. Probability of suffering of a biometric trait with changes is measured with permeance parameter.
- Collectability: It is a measure which expresses the specialized and human effectiveness in capturing the applicable characteristic data. A significant measured value provides user's solace and serves to choose for adoption or rejection of the biometric system.
- Performance: This parameter is linked with the time requirement. Execution of all required computations to carry out the biometric recognition in a given time, once the data is captured is referred as performance.
- Acceptability: It is the characteristic related to the users' social and cultural concerns, and in addition protection concerns associated with information capturing.
- Circumvention: The measure of difficulty to counterfeit a highly secure and reliable system is usually termed as circumvention.
- Trait Sensing: The capability of a system to sense or capture a particular biometric trait with accuracy and high speed is its trait sensing.

- Spoofing Difficulty: Acquiring data by falsing oneself as authentic person is referred as spoofing. This parameter measures for the difficulty in spoofing in percentage for a particular system.
- Speed and Cost Efficiency: This parameter refers to the processing and designing of the system i.e. the amount of time it takes to generate the output and implementation cost respectively.
- False Accept Rate (FAR): It is the probability measure of a system to inaccurately accept the unauthorized individual. Mathematically, it the ratio of number of false acceptances to the total number of identification attempts.

$$FAR = \frac{Number\ of\ false\ acceptances}{Total\ number\ of\ identification\ attempts} \tag{1.1}$$

- False Reject Rate (FRR): It is the probability measure of a system to incorrectly reject the authorized individual. Mathematically, it the ratio of number of false rejections to the total number of identification attempts.

$$FRR = \frac{Number\ of\ false\ rejections}{Total\ number\ of\ identification\ attempts} \tag{1.2}$$

Figure 1.7 and Table 1.1 illustrates a parameter based comparison between the most common biometric traits such as face, finger and palm print, finger and hand geometry, vein, iris, keystroke, retina, signature and voice or speech. The parametric percentage ranges between 0 and 100% corresponding to worst and best values in the considered biometric trait. The represented percentage values are obtained by averaging and weighting of parameters related to traits presented in [9], [23-34].

From Figure 1.7 and Table 1.1, it is observed that iris provides the best circumvention, spoofing difficulty, speed and cost efficiency, FAR and FRR when compared to other biometric traits. Iris also provides higher uniqueness values than other traits. Upon considering the points, a biometric recognition system based on iris could be thought to enhance. Hence in the work of present thesis biometric based Iris Recognition System (IRS) is implemented considering the previous researches and presented techniques that are discussed in further chapters to enhance the accuracy of the system and to attain major benefits in recognition field.

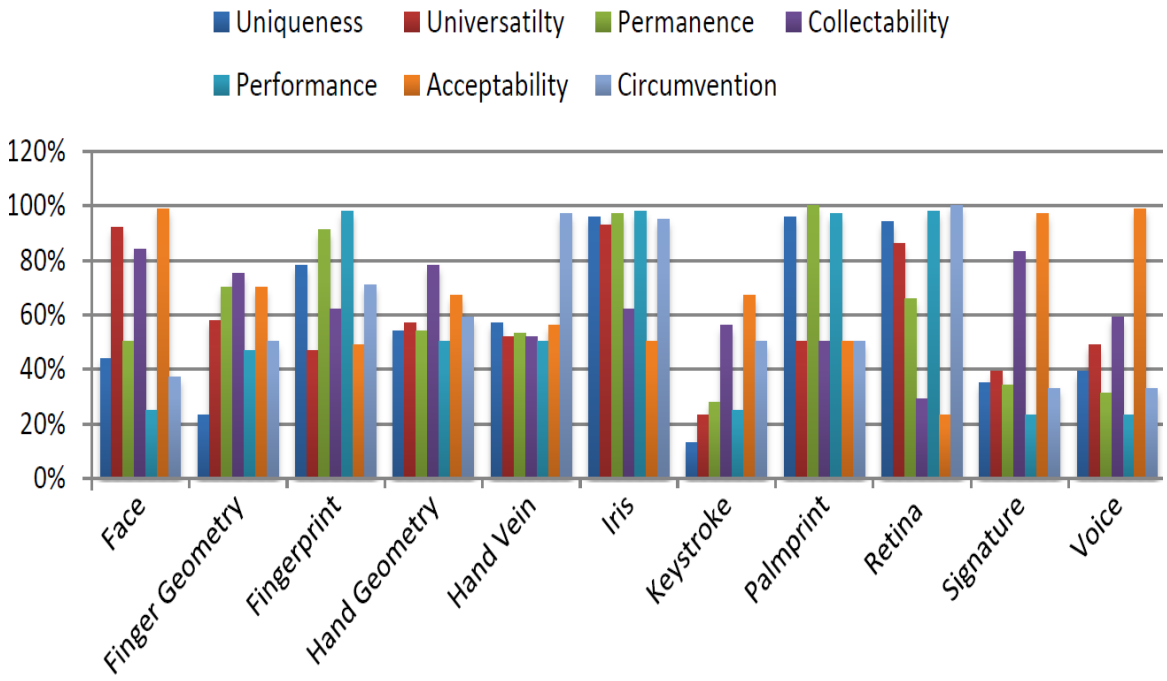

Figure 1.7: Parametric percentage vs biometric traits [9], [23-34]

Table 1.1: Parameter based comparison between the most common biometric traits [9], [23-34]

Parameters	**Face**	**Finger Print**	**Vein**	**Iris**	**Palm Print**	**Retina**	**Signature**	**Voice**
Uniqueness	Low	High	High	High	High	High	Low	Low
Permeance	Medium	High	High	High	High	High	Medium	Low
Circumvention	Medium	High	High	High	Medium	High	Low	Low
Trait Sensing	High	Medium	Medium	Medium	Medium	Medium	High	Medium
Speed and Cost Efficiency	Low	High	Medium	High	Medium	Medium	Medium	Low
Acceptability	High	Medium	Medium	Medium	Medium	Low	High	High
Spoofing Difficulty	Low	High	High	High	High	High	Low	Low
FAR	0.1 %	0.1 %	0.000008%	0.00001 %	0.114%	0-0.2%	5.5%	2-5 %
FRR	1.0-2.5 %	0.4 %	0.01%	0.02-0.14 %	0.012%	0-0.7%	2%	5-10 %

1.6 ORGANIZATION OF THESIS

The thesis work has been organized in the following chapters:

Chapter 2 Literature Review: An overview of human eye and its iris, IRS along with its steps of processing such as segmentation, normalization, feature extraction and feature matching is described in this chapter.

Chapter 3 Iris Localization, Feature Extraction and Matching: A method to enhance the eye image to make it suitable for post-processing is discussed in this chapter. Discussions about segmentation and normalization using Daugman's method over an eye image are also made. Feature extraction from an iris image based on various scanning techniques and Mean Square Error (MSE) method to match features for the final processing of IRS is then discussed in detail in this chapter.

Chapter 4 Results and Discussions: The various outcomes of image enhancement, segmentation, normalization, feature extraction and feature matching are presented in this chapter.

Chapter 5 Conclusion and Future Scope: The processing and observed results of the thesis are concluded here in this chapter and also the future work in this field is also suggested.

CHAPTER

LITERATURE REVIEW

2.1 INTRODUCTION

An eye of human body is photosensitive organ which is made up of three transparent layers. The outermost layer is fibrous tunic, consists of a curved frontal cornea and a larger unit sclera. The middle layer is known as vascular tunic, composed of choroid, ciliary body, iris and pupil. The innermost layer is retina [35]. The anatomy of the human eye is shown in Figure 2.1.

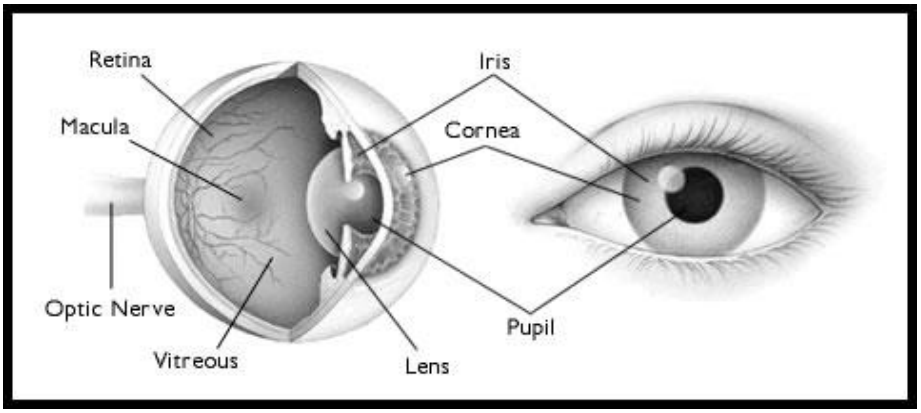

Figure 2.1: Anatomy of human eye [36]

The iris of the eye possesses a detailed and complex structure due to which it is considered as unique portion that can be used for the purpose of human identification. A brief description of iris is given in this chapter. Working and processing of IRS along with the methods required for its functioning are also explained in this chapter in brief context.

2.2 IRIS ANATOMY

Iris is the only internal part of the human body which is visible from outside around the pupil in human eye and it forms during the 3rd month of child's development in mother's womb via a process namely, chaotic morphogenesis [32]. It is a thin, circular structure and is almost similar to the diaphragm of the optical system of the body. It forms with the

combination of muscle cells, blood vessels, nerve endings, connective tissues and pigmented cells and all of these unitedly produce color patterns. Due to this, iris is seen as brown, green, blue, grey or hazel *etc* in color and hence, varies from person to person. Also it is said that the arrangement of blood vessels, pigmented cells *etc* is rich in details and form a unique pattern for each individual, hence can be used for non-invasive biometric authentication [37-39]. The iris anatomy is shown by Figure 2.2 which is indicating the complex structure of iris due to nerve fibers *etc*.

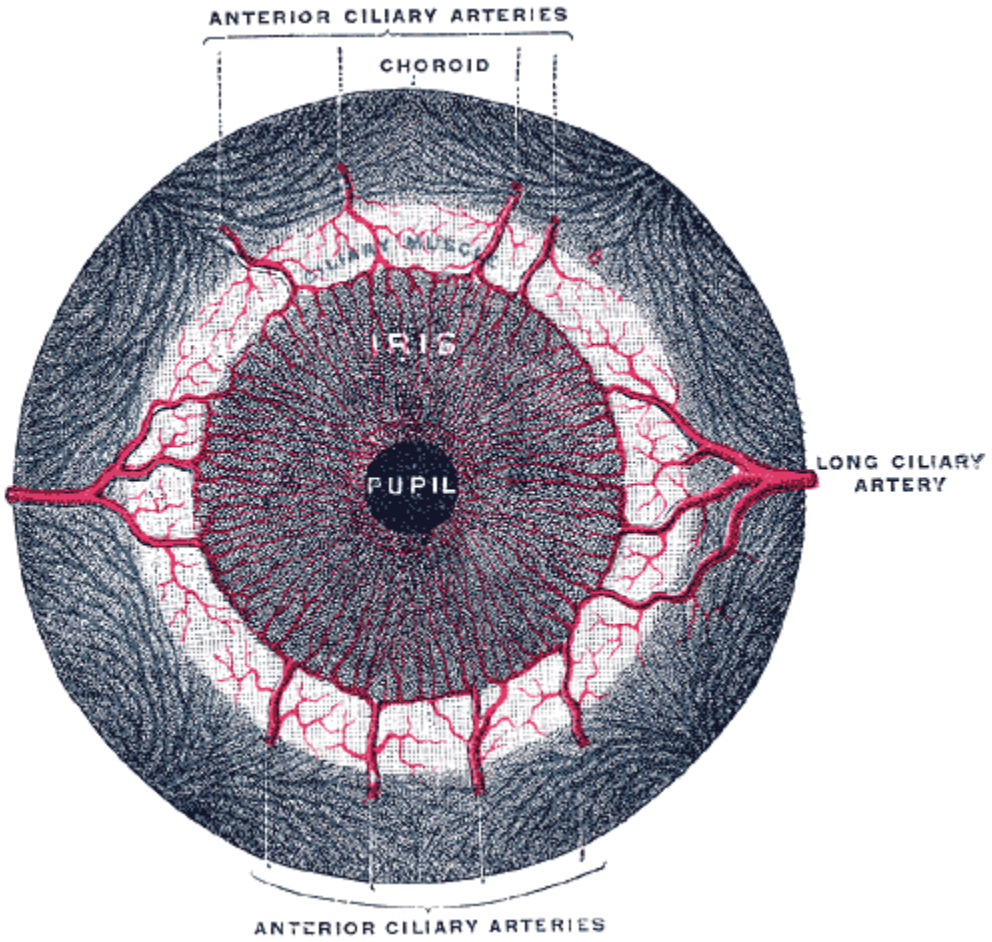

Figure 2.2: Anatomy of iris [40]

Among all other biometric patterns, iris patterns are said to be extremely complex. Also, iris is the most unique phenotypic visible feature available for easy and fast recognition of a particular's recognition [37]. The uniqueness of iris is said to be one in about 10^{31} people and for the same person, left and right iris differs with great value [41].

2.3 IRIS RECOGNITION SYSTEM

Recognition systems using biometric traits such as finger and palm prints, hand geometry, face, iris, retina, vein, signature, keystroke dynamics *etc* are explained in the previous chapter along with the comparison between them. From there it is concluded that among all, IRS provides the most promising biometric authentication and it is proved to be the most accurate and reliable when the acquired image quality is sufficiently good. IRS gets affected seriously with low quality due to motion, partial cooperation and user distance from scanner [42].

Iris recognition method for individual identification was originally proposed by ophthalmologist Frank Burch in 1936. In 1994, the basis for iris recognition and its underlying computer vision algorithms were patented by J.G. Daugman for image processing, feature extraction and feature matching [41].

Iris recognition is considered to be a very powerful technology in the field of recognition now-a-days. Some major points favoring the statement are as follows [32]:

- FAR and FRR for IRS is 0.02% and 0.00001% respectively.
- IRS possesses very high speed. Using ABIS7, it is possible to match 120million eyes/sec.
- Since size of the iris is very small, therefore it is possible to store 100million iris templates in 64 Giga Byte RAM i.e. 1.5 million iris templates/1 Giga Byte RAM.
- With high quality 2-eye iris system higher accuracy can be achieved rather than 10-fingerprint system.

Iris recognition is basically matching of features of iris and is done in five steps namely, eye image acquisition, segmentation, iris normalization, feature extraction and feature matching. The typical format of iris recognition is specified by the block diagram shown in Figure 2.3 and each block is briefly explained in following subsections.

2.3.1 EYE IMAGE ACQUISITION

The task of eye image acquisition with good visualization of iris is very hard due to many reasons like:

i) Iris is very small in size, usually only about 10 mms in diameter.

ii) Frequent movements of the eyeball.

iii) Light sensitive pupil.

iv) Uncooperative subject.

To reduce the effect of these factors, snapshot pictures from eye/iris acquisition video or near infrared camera is used to assure the high quality of iris image.

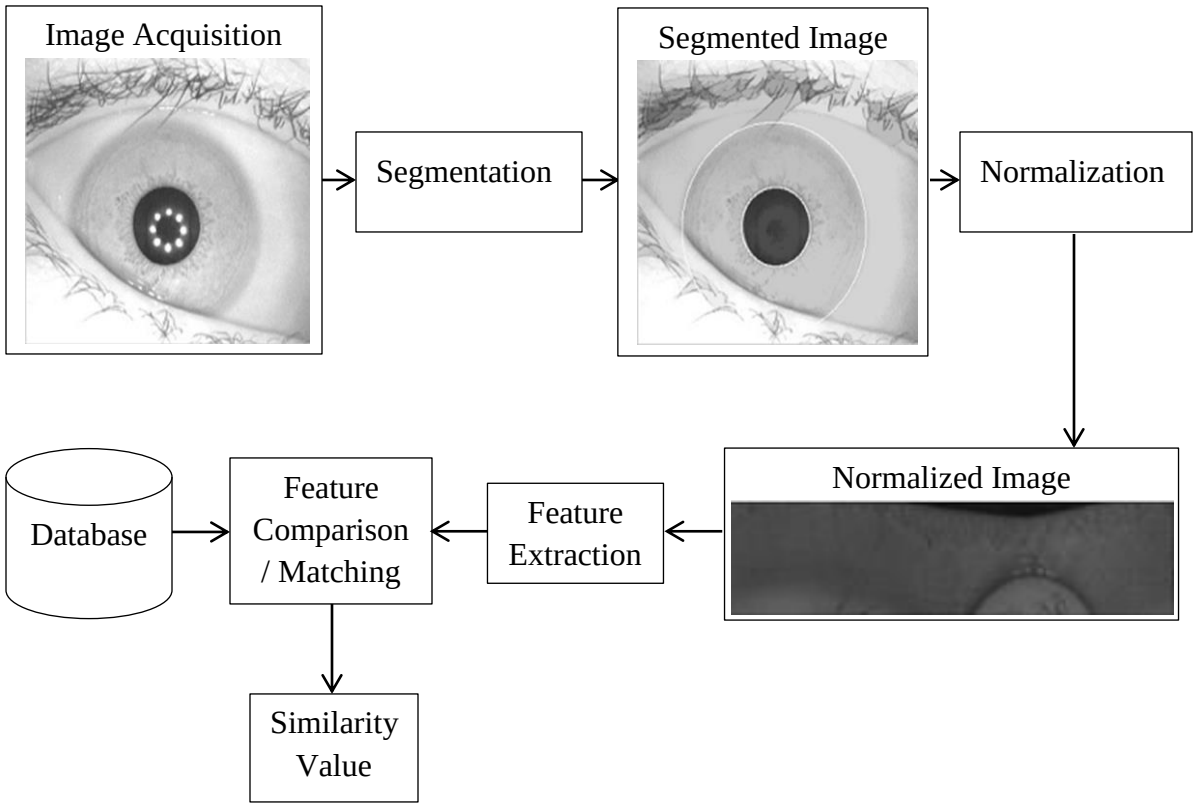

Figure 2.3: Block diagram of IRS [12]

2.3.2 IRIS SEGMENTATION

Segmentation means to divide the iris into segments or it is a method to separate the same eye's iris from the pupil. Segmentation of the iris image is a difficult task due to complex structure of iris image and also iris and pupil boundaries do not form perfect circles in many cases. An idea of iris segmentation can be taken from segmented image shown in Figure 2.3. Many segmenting techniques or methods have been introduced for the segmentation purpose that are described in following subsections.

2.3.2.1 DAUGMAN'S INTEGRO-DIFFERENTIAL METHOD

In 1993, Daugman presented one of the most relevant methods to perform the iris recognition. He proposed a method based on Integro-differential operator that was capable of searching for the circular pupil and the limbic borders of the iris in the eye image.

$$\max_{r,x_0,y_0} | G_\sigma(r) * \frac{\delta}{\delta_r} \oint_{r,x_0,y_0} \frac{I(x,y)}{2\pi r} ds | \tag{2.1}$$

where, $I(x, y)$ is the image area under consideration with coordinates x and y;

$G_\sigma(r)$ is the Guassian kernel;

r is the radius;

σ is the supreme convolution scale.

The Integro-differential operator given in equation 2.1 is a circular edge detector that searches for the parameters of a circular border and automatically localizes the iris region [41]. Processing of segmentation of iris is illustrated diagrammatically in Figure 2.4.

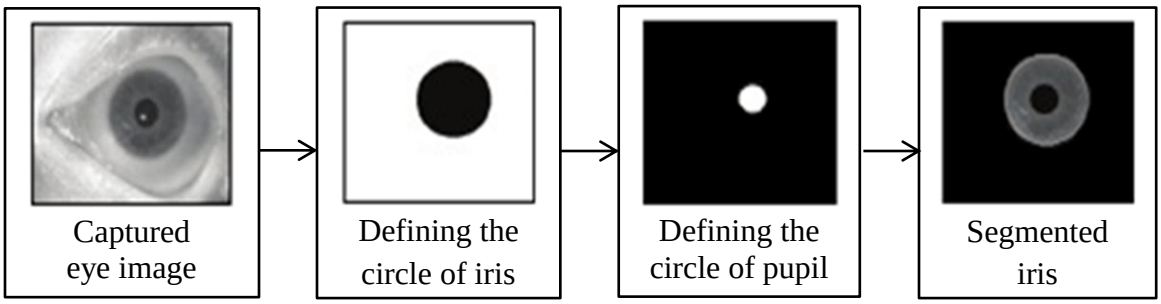

Figure 2.4: Processing of iris segmentation using Daugman's Integro-differential method [43]

2.3.2.2 HOUGH TRANSFORM

Hough Transform is a computer vision algorithm which is used to determine lines and circles present in an image. The radius and centre coordinates of the pupil and iris regions can be deduced using circular Hough Transform. An automatic segmentation algorithm based on the circular Hough Transform was presented by Wildes in 1997 [37]. He used the approach of segmenting iris through a gradient based binary edge map construction followed by Hough Transform. The initial step of the processing was to convert the

image intensity information binary edge map and so that the edge points could represent the contour parameter values. This operation was performed by thresholding the image intensity gradient,

$$|\nabla G(x,y) * I(x,y)| \tag{2.2}$$

where,

$$\nabla = \left(\partial/_{\partial x}, \partial/_{\partial y}\right) \tag{2.3}$$

and

$$G(x,y) = \frac{1}{2\pi\sigma^2} e^{\frac{(x-x_0)^2+(y-y_0)^2}{2\sigma^2}} \tag{2.4}$$

where, $G(x,y)$ is a 2-D Gaussian with center $(x_0, y_0)$and standard deviation σ.

Then Hough Transform is applied on the edge points (x_j, y_j) where, $j = 1,2, \dots n$, the center of the circle is assumed to be (x_c, y_c) and radius r,

$$H(x_c, y_c, r) = \sum_{j=i}^{n} h\left(x_j, y_j, x_c, y_j, r\right) \tag{2.5}$$

where,

$$h\left(x_j, y_j, x_c, y_j, r\right) = \begin{cases} 1, if\ g\left(x_j, y_j, x_c, y_c, r\right) = 0 \\ 0, \quad otherwise \end{cases} \tag{2.6}$$

and

$$g\left(x_j, y_j, x_c, y_c, r\right) = (x_j - x_c)^2 + (y_j - y_c)^2 - r^2 \tag{2.7}$$

The edge points that are located over the circle results 0 value of h-function whereas value of g becomes 1, represents the local pattern of contour [37]. Diagrammatic representation of processing of the operator is shown in Figure 2.5.

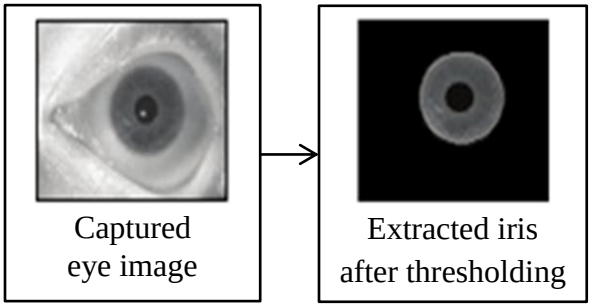

Figure 2.5: Processing of iris segmentation using Hough Transform [43]

2.3.2.3 DISCRETE CIRCULAR ACTIVE CONTOUR METHOD WITHOUT RE-INITIALIZATION

Discrete active circular contour method without re-initialization initially was proposed by Li *et al*. [44]. Singh *et al.* [12] implemented the method on iris images to localize the iris region accurately for iris recognition purpose. This method detects the pupil and limbus boundary based on two types of energies *i.e.* internal and external energy.

The processing of the iris segmentation using discrete circular active contour method without re-initialization is shown in Figure 2.6.

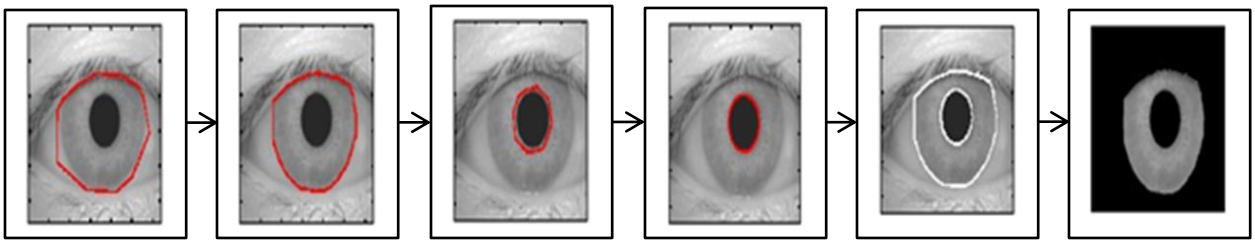

Figure 2.6: Processing of iris segmentation using discrete circular active contour method without re-initialization [12].

The problem related to this method is that the initial contour for each eye is to be defined manually.

2.3.2.4 CANNY EDGE DETECTION AND K-MEANS ALGORITHM

Jayachandra *et al*. [45] introduced canny edge detection and K-means algorithm in 2013. According to which, canny edge detection method focuses on pupil edge detection in iris recognition to reduce the noisy data from images and detects the edges. After edge detection, images are stored in database and then K-means algorithm is applied to recognize an image from database that possesses nearest pupil edge for the given input image.

2.3.2.5 COMPARISON BETWEEN THE SEGMENTATION TECHNIQUES

To analyze the significant performance of segmentation techniques a comparison is presented in Table 2.1 which provides the accuracy percentage of the segmentation techniques. On the basis of this comparison a segmentation method is selected for the processing of current thesis work.

Table 2.1: Comparison between segmentation techniques [12], [46]

Method	**Accuracy Percentage**
Daugman's Integro-differential Operator Method	87%
Hough Transform	83%
Discrete Circular Active Contour Method without Re-initialization	99.20%
Canny Edge Detection and K-means Algorithm	83.95%

2.3.3 IRIS NORMALIZATION

After segmentation of both the inner and outer boundaries of the iris, normalization process is to be done to fix the dimensions of the iris region in order to do comparisons. The captured images of irises may have different sizes due to variation in pupil size which depends on variation of illumination, distance and angle of image capturing. The variation in size of irises can lead to higher complexity in recognition task. Hence, for ease and accuracy, the segmented iris data should be invariant to the dimensions. To resolve the problem, various normalization methods have been introduced till date.

Daugman's Rubbersheet model is the most common method used for the purpose of normalization. It was proposed by Daugman in 1993. In this case, segmented iris images in the cartesian coordinate system (x, y) are transformed to fixed length and dimensionless polar coordinate system (r, θ) using pupil's centre as a reference point [41], [47] for an iris image *I*.

$$I\big(x(r,\theta), y(r,\theta)\big) \rightarrow I(r,\theta) \tag{2.8}$$

where, $x(r,\theta)$and $y(r,\theta)$ are the linear combinations of both pupillary boundary points $(x_p(\theta), y_p(\theta))$ and sclera boundary points $(x_s(\theta), y_s(\theta))$ which are detected during iris segmentation.

Another method introduced by Wildes in 1997 [37] is image registration method which is capable to deform an iris image. This method searches for a transformation which maps each point of acquired image $I_a(x, y)$ into an alignment with selected database image $I_d(x, y)$ in accordance with mapping function $(u(x, y), v(x, y))$. The

newly acquired image intensity values are made to be close to corresponding points in the selected database image.

Virtual circles method given by Boles *et al*. in 1998 [48] is another technique to perform normalization. Initially all iris images are scaled to a reference annular zone, which is the ratio of the radii of inner and outer boundaries of the iris non-linearly and then unwarp this annular zone to a fix-sized rectangle block linearly for subsequence processing [13]. This works differently than other techniques since normalization is not performed until two iris regions match. When two irises are considered to have same dimensions, feature extraction is done from iris region by storing the intensity values along with the virtual concentric circles taking origin at center of pupil. To extract same number of feature coefficients from each iris image matrix, normalization resolution is selected.

2.3.4 FEATURE EXTRACTION

Feature extraction is an important part of IRS to extract out the required and important features out of the normalized iris image. Some methods that have been considered by various researchers for the process of the feature extraction are briefly explained as follows:

Nichal *et al.* [49] introduced an iris feature extraction method based on Discrete Cosine Transform (DCT) and the differences of DCT applied matrix coefficients from normalized iris images are then used for coding and matching. Abhiram *et al*. [50] also used DCT over normalized iris images to concentrate significant features towards upper-left corner of coefficient matrix and extracting required feature coefficients. The DCT for a 2-D image F_{uv} is given by following equation [51],

$$F_{uv} = \beta_u \beta_v \sum_{m=0}^{M-1} \sum_{n=0}^{N-1} P_{mn} \cos\frac{\pi(2m+1)u}{2M} \cos\frac{\pi(2n+1)v}{2N} \tag{2.9}$$

$$\beta_u = \frac{1}{\sqrt{M}} \text{ if } u = 0 \qquad \beta_v = \frac{1}{\sqrt{N}} \text{ if } v = 0$$

$$= \sqrt{\frac{2}{M}} \text{ if } 1 \le u \le M-1 \qquad = \sqrt{\frac{2}{M}} \text{ if } 1 \le v \le N-1 \tag{2.10}$$

where, F_{uv} are known as the DCT coefficients of 2-D normalized image given as $P(m, n)$.

Elementary frequency components of a signal are decomposed by DCT. The 2-D DCT concentrates the significant energy information of $M \times N$ matrix in a few coefficients in upper-left corner of resulting $M \times N$ DCT matrix.

According to Panganiban *et al.* [52], using wavelet transform method, the normalized iris image is decomposed into N levels (where, max. N=4). After applying wavelet transform the image will be divided into 4 sub-images, from which low frequency components are extracted to encode so as to have the discriminating information content from the iris image.

The Fast Wavelet Transform (FWT) is a mathematical algorithm designed to convert a waveform or a signal in the time domain into a sequence of coefficients based on an orthogonal basis of small finite waves, or wavelets and also to extract the low frequency unique features. Oluwakemi *et al.* [53] suggested that the transform can be applied to multidimensional signals, such as images, where the time domain is replaced with the space domain. Hence, in IRS when FWT is applied over normalized iris image, unique feature are extracted and are then coded for the matching purpose.

Khan *et al.* [54] suggested the use of 1-D Gabor filter to extract unique feature information from iris. 1-D Gabor filter provide real and imaginary feature coefficients, extracts the unique features from the iris (known as iris code) in the form of coefficients and then store them.

A modification of basic Gabor filters known as Log-Gabor function, provides advantageous results filters over complex basic Gabor filters. According to Yao *et al.* [55], Log-Gabor filter is strictly bandpass filter. Iris feature extraction appears to be more suitable due to this property regardless of the background brightness.

Nisar *et al.* [56] gave a method in which feature extraction process is to be done in two steps separately in two phases *i.e.* training phase and testing phase. Initially, the image signal is converted to 1-D signal which was in 2-D previously and then feature extraction is done using Mel Frequency Cepstral Coefficient (MFCC). The purpose of working with two phases solves during matching as the sample features which were

saved in database in the training phase are matched with the testing phase extracted feature [56].

2.3.5 SCANNING PATTERNS

The Feature Vector (FV) coefficient matrix obtained after applying DCT (which concentrates the significant energy of a matrix in a few elements towards the upper-left corner of the matrix) over the normalized iris matrix, and then fed to undergo scanning procedures. The scanning procedures can follow various scanning patterns designed on the basis of Space Filling Curves (SFC) *i.e.* to consider an element for only once of a matrix. Some of the commonly used scanning patterns by researchers for any image to extract coefficients or features are Zigzag, Raster and Sawtooth patterns. Brief description of these patterns is as follows:

2.3.5.1 MATRIX PATTERN

When DCT is applied over 2-D image, it concentrates the energy towards upper-left corner of the image. Hence Kekre *et al*. [51] proposed a varying matrix size selection method as shown in Figure 2.7 to use only those upper-left coefficients and discard the remaining coefficients so as to take the benefit of matching for recognition purpose from a very few coefficients instead of considering the whole iris image matrix.

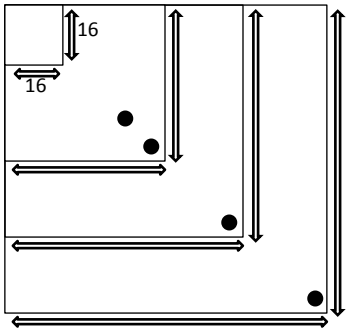

Figure 2.7: Varying matrix size selection method

2.3.5.2 ZIGZAG PATTERN

According to Bradley [57], Zigzag scan came in existence from Z-pattern layout that follows the shape of letter ‘z’ as shown in Figure. 2.8. When ‘z’ letter is extended to series of pattern, resultant pattern is referred to as Zigzag pattern as shown in Figure 2.9.

Bhatnagar *et al*. [58] also explained the zigzag scan pattern on the basis of letter Z-pattern as SFCs in an image.

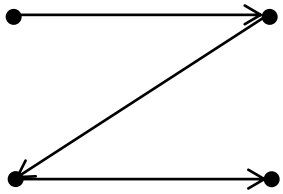

Figure 2.8: Z-pattern

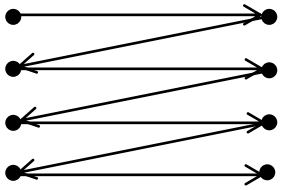

Figure 2.9: Zigzag pattern

2.3.5.2 RASTER PATTERN

Bhatnagar *et al.* [58] explains the scanning patterns on the basis of SFCs that traverse every element of the matrix exactly once. Raster pattern is explained as rectangular path traversing an image as shown in Figure 2.10.

2.3.5.3 SAWTOOTH PATTERN

Sawtooth pattern is also explained by Bhatnagar *et al.* [58] in context with SFC method. Its pattern is similar to the sawtooth wave or curve as shown in Figure 2.11 and is capable of traversing each element for just once of an image in similar manner as in Zigzag and Raster scan pattern.

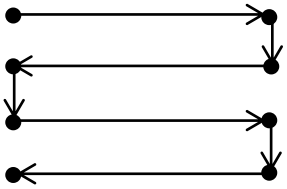

Figure 2.10: Raster pattern

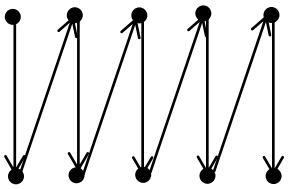

Figure 2.11: Sawtooth pattern

Alike patterns are then used in undertaken work to recognize the iris.

2.3.6 FEATURE MATCHING

For the matching purpose, comparison will be done between the in-hand encoded iris image and the iris images present in the dataset. It is the last level of the iris recognition process which could be performed using various techniques as described following.

Hamming Distance (HD) is the most familiar method for the matching purpose of the bit pattern formed after coding of the extracted FV of input iris sample and iris from the database available. The validation check is done by use of EX-OR function operator.

$$H.D. = \frac{1}{N}\sum_{j=i}^{N} X_j \otimes Y_j \tag{2.11}$$

where, X represents the bit pattern of input iris sample;

Y represents the bit pattern of iris sample present in database.

Weighted Euclidean Distance (WED) is another method used to compare two integer valued templates and to have the measure of similarity of collection of values between two templates.

$$WED(k) = \sum_{i=1}^{N} \frac{(f_i - f_i^{(k)})^2}{(\delta_i^{(k)})^2} \tag{2.12}$$

where, f_i is the i^{th} feature of unknown iris;

$f_i^{(k)}$ is the i^{th} feature of iris template k;

$\delta_i^{(k)}$ is standard deviation of i^{th} feature of iris template k.

Matching between scanned FV matrices of each normalized iris in the testing data set with complete training data set in the database can also be performed by applying Mean Square Error (MSE) formula over them to recognize the individual from the database. For every training image $'x'$ and test image $'y'$ MSE is calculated using equation 2.24 [32],

$$MSE(x) = \frac{1}{3M^2}\sum_{m=0}^{M-1}\sum_{n=0}^{N-1}\sum_{d=0}^{2}[FV_x(m,n,d) - FV_y(m,n,d)]^2 \tag{2.13}$$

where, $M$and N represents the size of the FV matrix. Initially, $M = N = 100$.

The trainee image with least MSE is indicated as the identified individual. Matching process is repeated for the varying size of scanned FV matrix.

2.4 MOTIVATION

For the processing of IRS, segmentation of eye image and normalization of localized iris from the eye image performs a major role. Therefore, it is necessary to perform these steps. The segmentation and normalization techniques *i.e.* Daugman's Integro-differential

operator and Daugman's Rubbersheet model, respectively, provide the best results among all other techniques. Hence, they are used for the initial processing of the proposed work. For feature extraction, DCT have been used previously with matrix method employment. It is observed that feature coefficient extraction based on various scanning techniques after the application of DCT over normalized iris has not been employed and checked. So a work in this direction is to be done. Since, for the complete processing of IRS feature matching is also required, being simple and easy, a method named MSE is to be used in this step.

2.5 THESIS OBJECTIVE

The objective of the thesis is,

1. To perform feature extraction based on various scanning techniques after applying DCT on the normalized iris image.
2. To perform feature matching using MSE method between training data and test image.

2.6 DATABASE

For biometric research and development, analysis of human data is required. It is more relevant to take test data of the same trait and of the same specie for which the system has to perform to achieve fair results. Therefore, for testing of recognition methods, biometric databases with very high relevance are prepared as an indispensable material.

Institute of Automation under Chinese Academy of Sciences actively researches on the topic of iris recognition. To analyze the various algorithms based on iris recognition CASIA has developed iris image databases. This database is very popular among the researchers and is commonly used in the iris recognition field.

We have used CASIA database version-IV for the purpose of our research [59]. The 8-bit grey level JPEG iris images are collected under infrared illumination with novel designed camera to capture very clear iris images that includes detailed texture features of iris in indoor environment. Very close and homogeneous characteristics are possessed by the iris images in the database. Obstructions caused by eyelids and eyelashes are referred to as noise factors in the iris images. The resolution of the images is 320×280.

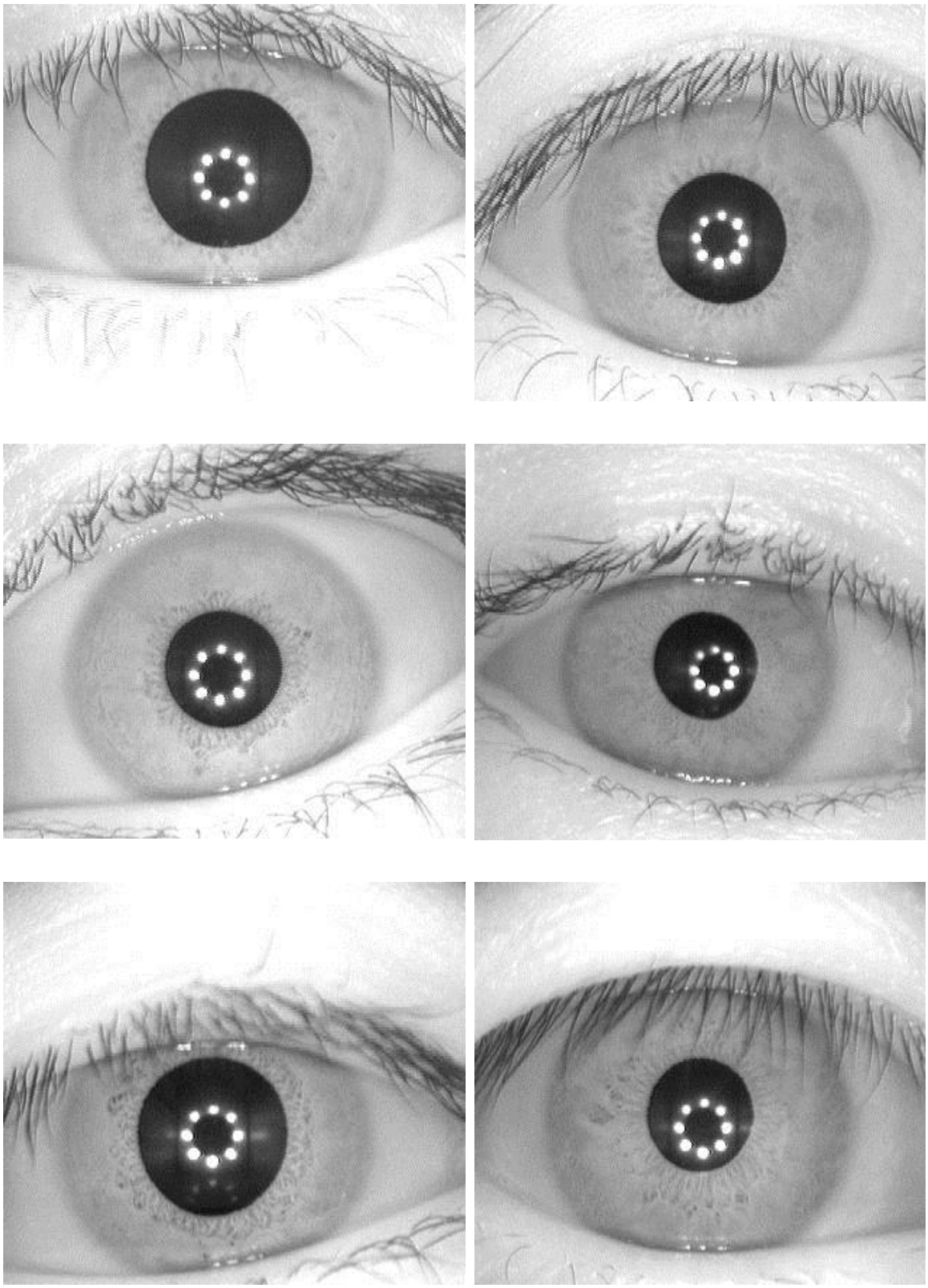

Figure 2.12: Examples of iris images from CASIA database version-IV

2.7 SUMMARY

In this chapter the basis and basics of IRS are discussed along with the techniques and methodologies required for its processing. In the proposed work database was required to perform the testing, hence brief detailing of the CASIA database is provided which is to be used in the work for correct processing. Some of the eye images from the database are also presented as examples for its better understanding. To fulfill the thesis objective, the discussed details in the chapter are taken as base for processing of the proposed work which is presented in the next chapter.

CHAPTER

IRIS LOCALIZATION, FEATURE EXTRACTION AND MATCHING

3.1 INTRODUCTION

Various steps are required to be followed in iris recognition. These steps and the related methodologies are already explained in brief in the previous chapter. This chapter involves the operations and methods *i.e.* segmentation using Daugman's Integro-differential operator, normalization using Daugman's Rubbersheet model, feature extraction based on various scanning techniques and feature matching using MSE for iris recognition, considered under the work of thesis. The methods used for the processing are explained in detail in this chapter.

3.2 COUNTERING THE EFFECT OF LIGHT REFLECTIONS

For iris recognition the first step to be taken after image acquisition is segmentation. Since the segmentation process that is to be taken under consideration for this work is Daugman's Integro-differential operator method. This method has a limitation that it is not capable to perform well when extra light effects or reflections are present in the eye image [31]. Therefore, to overcome this limitation a step before segmentation is performed which is referred as countering the effect of light reflections. Also, there is a requirement of setting threshold level on pixel intensity values over which the operator is to be applied to reduce the time as well as computational complexity.

Figure 3.1 (a) and (b) shows the eye images from the database having light reflections that fall on the images while capturing the images. The white ovals in the images enclose the area having light reflections in the image.

3.2.1 REFLECTION REMOVAL

Since the reflection removal is necessary for fine functioning of IRS, therefore MATLAB command 'imcompliment' and 'imfill' are used before applying Daugman's operator to

the image. On applying the commands as required, the visible changes in an image after reflection removal can be observed from the Figure 3.2.

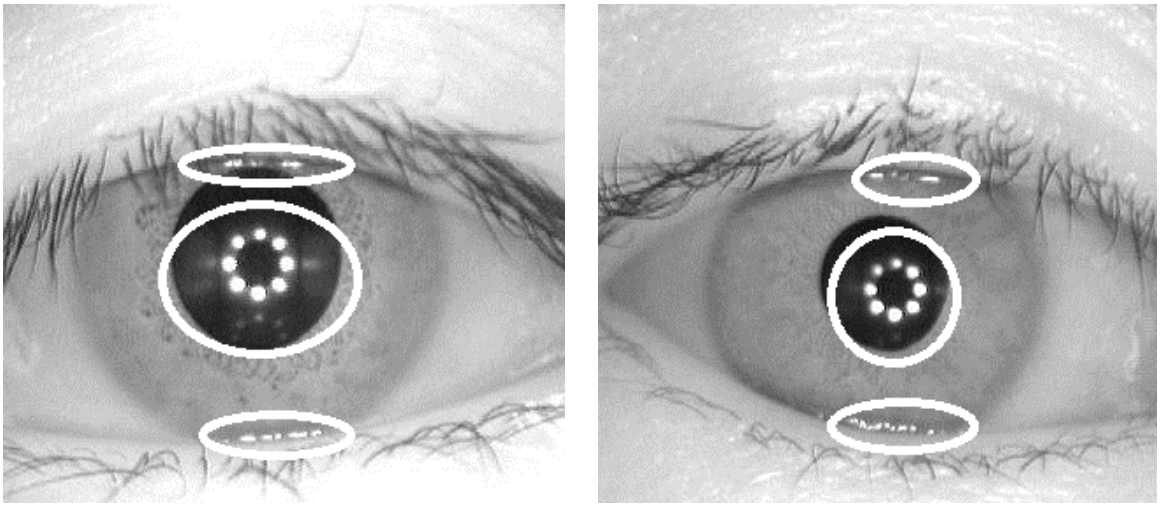

(a) (b)

Figure 3.1: Depiction of light reflection in eye images

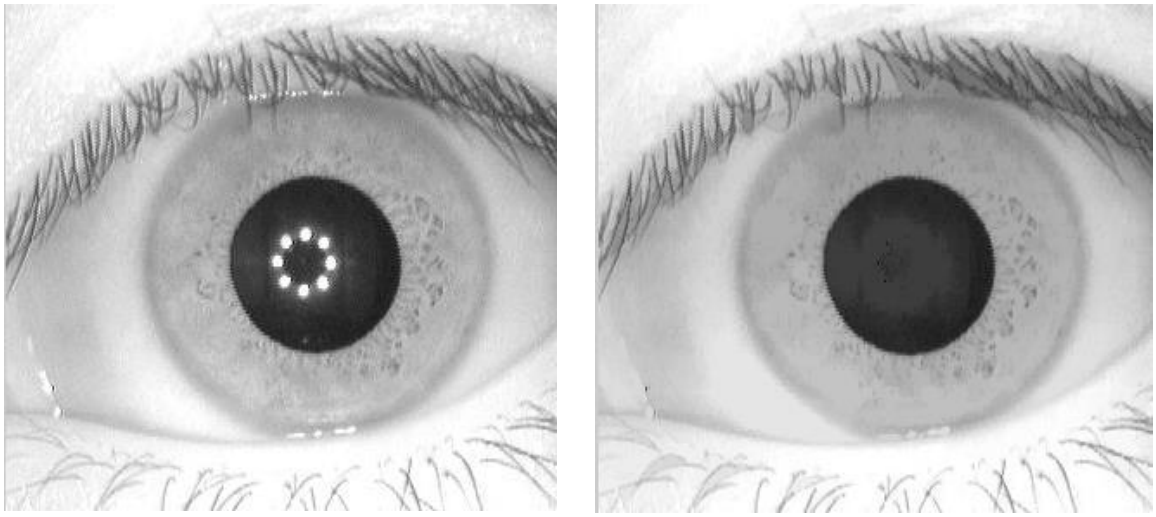

(a) Eye image (b) Eye image after reflection removal

Figure 3.2: Removal of reflections from original eye image

3.2.2 THRESHOLDING

After the reflection removal from the eye image, thresholding is to be done. 'Thresholding below' method is used to get an area from the image where the center pixels may lie. In presented work, the object pixels (*i.e.* the pixels that could possibly be the center pixels) have been assumed to have a value below 0.5 [31]. So, all the pixels

that have intensity value less than 0.5 are marked and the Daugman's operator is applied on those pixels only.

3.2.3 DETECTING PIXELS WITH LOCAL MINIMUM VALUES

The threshold image is further scanned, pixel by pixel to determine whether the pixel is a local minimum in that particular pixel's immediate 3×3 neighborhood. This means that each pixel's intensity is compared to the intensities of the pixels in the immediate nine neighborhood pixels. The pixel with lowest intensity value amongst these nine pixels is used for further calculations. The rest of the pixels are discarded.

The reduction in the number of object pixels, on which Daugman's operator is applied, makes the iris detection process faster.

3.3 DAUGMAN'S SEGMENTATION METHOD

After performing the above steps, extraction of iris is required and for this Integro-differential operator is used that searches for the circular pupil and limbic borders of the iris in the eye image using the equation [41],

$$\max_{r,x_0,y_0} | G_\sigma(r) * \frac{\delta}{\delta_r} \oint_{r,x_0,y_0} \frac{I(x,y)}{2\pi r} ds | \tag{3.1}$$

The Daugman's operator looks over the image domain (x, y) for uttermost in the blurred by a Gaussian kernel $G_\sigma(r)$ partial derivative w.r.t. increasing radius r, of normalized contour integral of $I(x, y)$ throughout a circular arc ds of radius r and center coordinates (x_0, y_0). This method searches in N^3 space for center, radius and circumference with highest derivative values comparing to circumference of neighbor radius [12]. Initially, the blurring factor σ is set for a rough scale of perusal so as only very distinct circle transition from iris to sclera is detected. Then after this strong circular boundary is more accurately estimated, a second search begins for the indistinct pupillary boundary within the confined region of iris, using supreme convolution scale σ and a smaller search range defining paths (x_0, y_0, r) contour integration. For rapid discrete implementation of Integro-differential operator in equation 3.1, it is more efficient to interchange the order of differentiation and convolution and concatenate them before computing the discrete convolution of the resulting operator with discrete series of under sampled sums of pixels

along with circular contours of increasing radius. Using finite difference approximation, to the derivative for the discrete series in n,

$$\frac{\partial G_\sigma(r)}{\partial r} \cong G_\sigma^1 = \frac{1}{\Delta r} G_\sigma(n\Delta r) - \frac{1}{\Delta r} G_\sigma((n-1)\Delta r \tag{3.2}$$

where, Δr is a little increase in the radius and by replacing the convolution and contour integrals with sums, we can derive through these manipulations a methodical discrete operator for finding the inner and outer borderlines of the iris. $\Delta\theta$ is angular sampling interval along circular arcs, over which the summed $I(x, y)$ pixel intensities represent the contour integrals expressed in equation 3.1. For CASIA database, values of iris radius and pupil radius ranges from 90 to 150 and 28 to 75 pixels respectively [12]. Daugman's segmentation result for eye images of two different persons is shown in Figure 3.3.

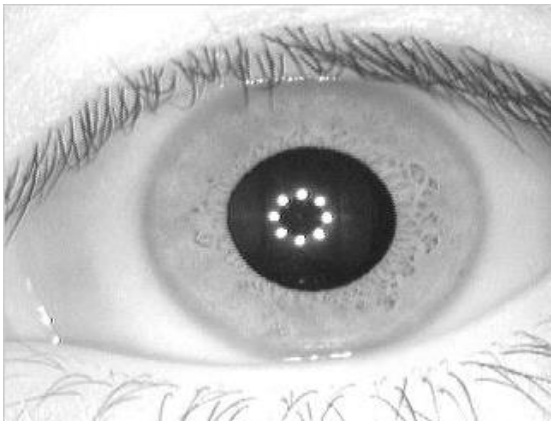

(a) Eye image of person-1

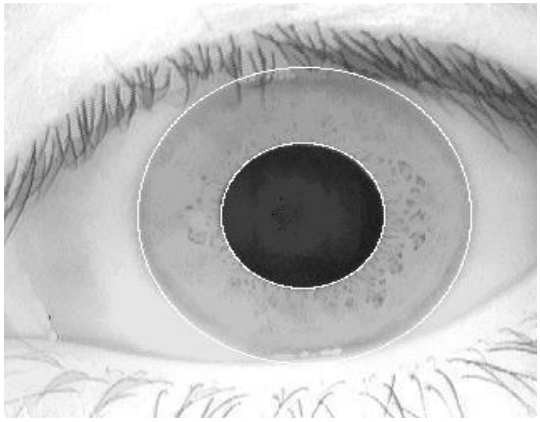

(b) Segmented eye image of person-1

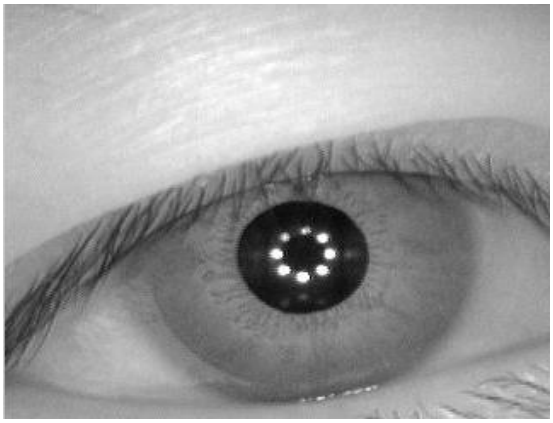

(c) Eye image of person-2

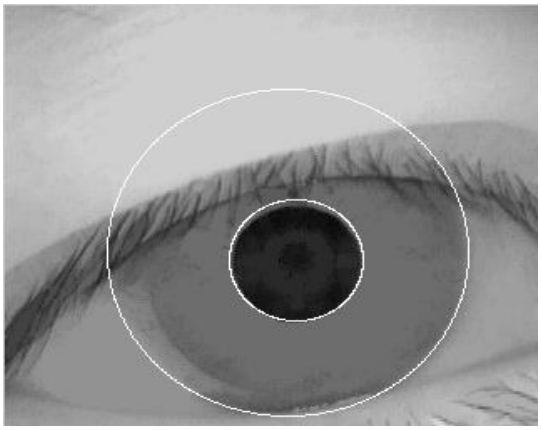

(d) Segmented eye image of person-2

Figure 3.3: Illustration of segmented eye image

3.3.1 DAUGMAN'S SEGMENTATION METHOD WITHOUT REMOVING LIGHT REFLECTIONS

When Daugman's Integro-differential operator is introduced to an eye image without removing the light reflections then the light reflections creates hindrance in iris detection process as shown in Figure 3.4.

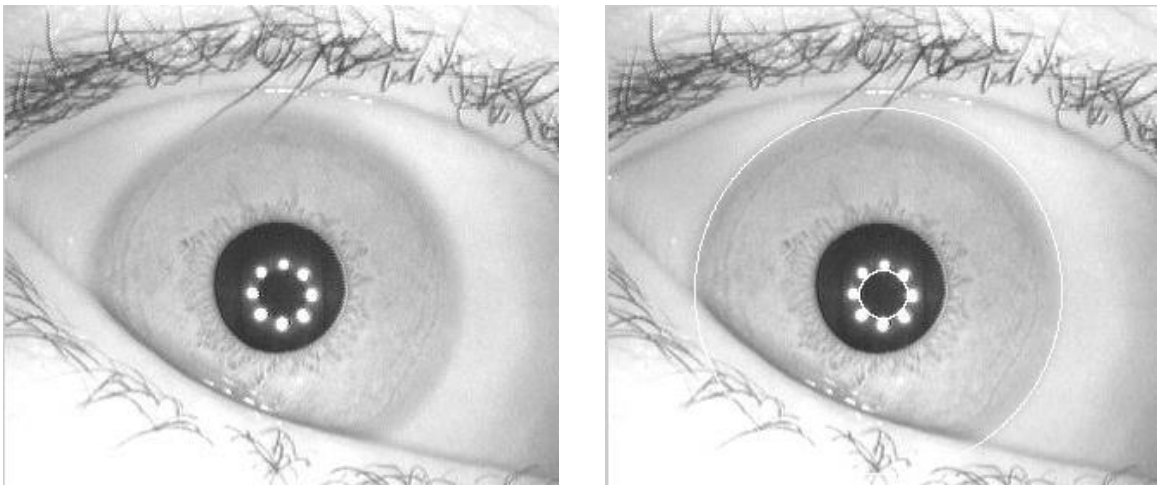

(a) Eye image (b) Wrongly detected circles in the eye image

Figure 3.4: Illustration of wrongly segmented eye image

3.4 NORMALIZATION

In normalization, for comparison purpose, the extracted iris region is mutated to have fixed dimensions. This method is used to achieve good detection. Illumination variations results in change of pupil size, which ultimately causes elastic deformations in iris texture. This elastic deformation causes problem in pattern matching. So, to achieve accuracy in analysis, it is necessary to compensate the deformation. J.G. Daugman [41] introduced Rubbersheet model to normalize the iris that changes an image in cartesian coordinates (x, y) to image in polar coordinates (r, θ) with fixed dimensions by countering pupil dilation effect as shown in Figure 3.5.

After performing segmentation using Daugman's Integro-differential operator to localize the iris region from eye image and normalization using Daugman's Rubbersheet model to have fixed dimension matrices for all extracted iris matrices, experimental

results are obtained. From these, results for a person from the used database are shown in the Figure 3.6.

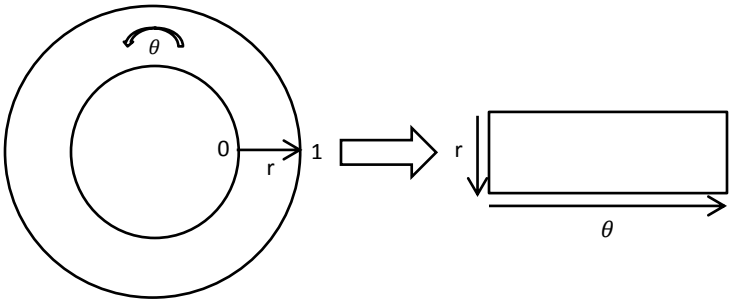

Figure 3.5: Daugman's Rubbersheet model [45]

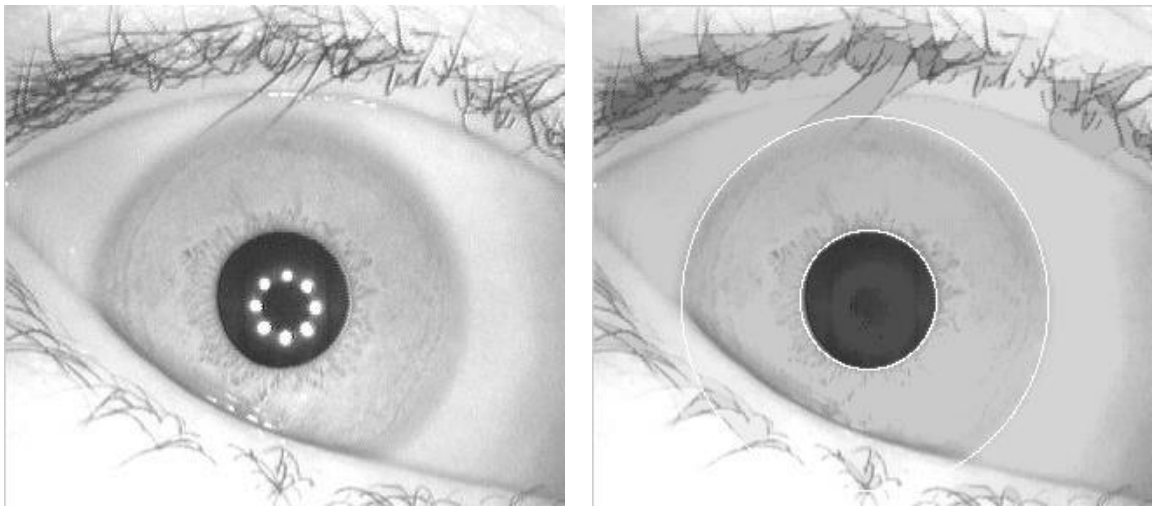

(a) Eye image of person-1 (b) Segmented eye image of person-1

(c) Normalized extracted iris of person-1

Figure 3.6: Experimental illustration of localized and normalized iris image

3.5 FEATURE EXTRACTION

In order to use iris pattern for recognition purpose, it is paramount to define a depiction that is well adapted for extracting the iris information content from normalized iris [60].

Hence, feature extraction is known to be an important part of IRS as important features are required to be extracted from the normalized iris image.

3.5.1 DISCRETE COSINE TRANSFORM

After normalizing the entire database images to be used as training image or as testing image, the fourth step will then be performed by applying DCT to the normalized iris image matrices. The DCT for a 2-D image F_{uv} is given by following equation [51],

$$F_{uv} = \beta_u \beta_v \sum_{m=0}^{M-1} \sum_{n=0}^{N-1} P_{mn} \cos\frac{\pi(2m+1)u}{2M} \cos\frac{\pi(2n+1)v}{2N} \tag{3.3}$$

$$\beta_u = \frac{1}{\sqrt{M}} \text{ if } u = 0 \qquad \beta_v = \frac{1}{\sqrt{N}} \text{ if } v = 0$$

$$= \sqrt{\frac{2}{M}} \text{ if } 1 \le u \le M-1 \qquad = \sqrt{\frac{2}{M}} \text{ if } 1 \le v \le N-1 \tag{3.4}$$

where, F_{uv} are known as the DCT coefficients of 2-D normalized image given as $P(m,n)$.

Elementary frequency components of a signal are decomposed by DCT and 2-D DCT concentrates the significant energy information of $M \times N$ matrix in a few coefficients towards upper-left corner of resulting $M \times N$ DCT matrix which is then considered as FV matrix..

3.5.2 SCANNING TECHNIQUES

From the obtained FV matrix after application of DCT, it is convenient to extract only those coefficients having maximum energy so that motive of matching can be solved using them only in place of using the whole FV matrix. This helps in reduction of computational complexity for the system. To extract the partial coefficients, methods of scanning used are Zigzag, Raster Type-I, Raster Type-II, Sawtooth Type-I, Sawtooth Type-II and Sawtooth Type-III [57-58] as shown in the Figure 3.7.

The complete experiment is performed over the total of 198 iris images. From these 198 iris images, the training set comprises 132 images and test data set comprises 66 images.

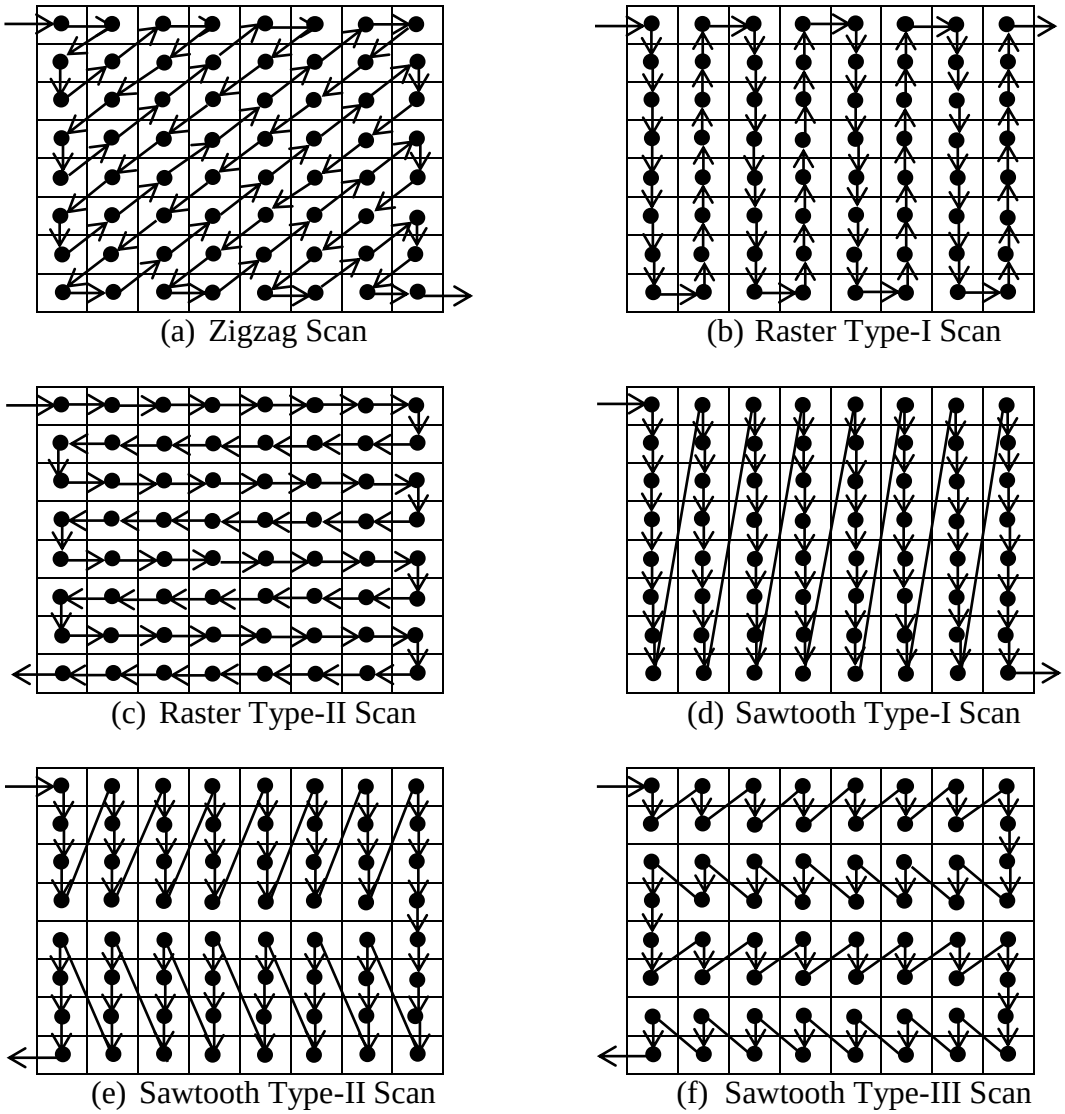

(a) Zigzag Scan (b) Raster Type-I Scan

(c) Raster Type-II Scan (d) Sawtooth Type-I Scan

(e) Sawtooth Type-II Scan (f) Sawtooth Type-III Scan

Figure 3.7: Various scanning techniques

3.6 FEATURE MATCHING

The scanned FV matrices of each normalized iris in the testing data and the training set is performed by applying the MSE formula over them to recognize the individual. For every training image $'x'$ and test image $'y'$ MSE is calculated using [51],

$$MSE(x) = \frac{1}{3M^2} \sum_{m=0}^{M-1} \sum_{n=0}^{N-1} FV_y(m,n) - FV_y(m,n)]^2 \tag{3.5}$$

where, $M$and N represents the size of the FV matrix. Initially, $M = N = 100$.

An individual is said to be identified when obtained MSE is minimum for a trainee image. Matching process is repeated for the varying size of scanned FV matrix.

3.7 SUMMARY

In this chapter, the steps followed for the processing of proposed IRS such as countering the effect of light reflections, thresholding to reduce time and computational complexity, segmentation using Daugman's Integro-differential method, normalization using Daugman's Rubbersheet model, feature extraction based on various scanning techniques and feature matching using MSE method are explained in detail. The observed results are presented in the next chapter along with the discussions related to them.

CHAPTER

RESULTS AND DISCUSSIONS

4.1 INTRODUCTION

The automatic segmentation using Daugman's Integro-differential operator proved to be successful when analyzed over CASIA iris database version-IV. Briefly, when Daugman's Integro-differential operator was applied on the images from database for segmentation, iris region is localized assuming iris and pupil to be perfect circles, sclera portions and iris pupil boundaries were clearly distinguished. After localization, iris regions are extracted from the eye images and normalized using Daugman's Rubbersheet model. This model converts the iris images into polar coordinates (r, θ) obtained from the cartesian coordinates (x, y). Partial FV coefficients are then extracted using scanning techniques after application of DCT over the normalized iris matrices and generates FV coefficient matrices for all irises in training as well as in testing sets. Feature matching is then performed to recognize the iris in training set and matching percentage is recorded for test set images. In this chapter, experimental results of light countering, segmentation, normalization, accuracy analysis prepared after matching, comparison with the existing technology and complexity analysis of the system is presented.

4.2 EXPERIMENTAL OBSERVATIONS OF LIGHT REFLECTION COUNTERING, SEGMENTATION AND NORMALIZATION

When the eye image input is given to the system, then the first necessary step is to counter the light effects and reflections from the image so that proper segmentation can be achieved through Daugman's operator to localize the iris. After segmentation, localized iris region is then normalized to make it independent of the dimensions. The observed experimental results after countering the light effects, segmentation and normalization for four eye images are shown in Figure 4.1.

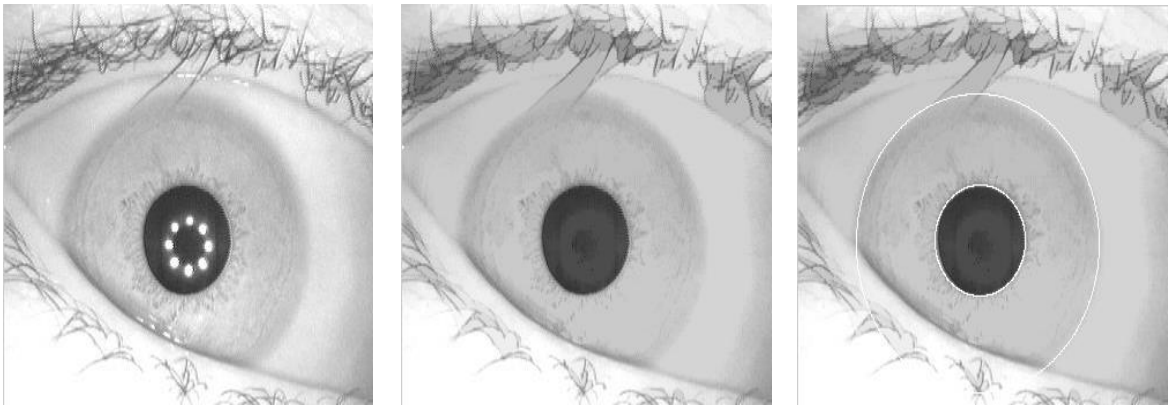

(a) Eye image of person-1 (b) Eye image with countered light reflections (c) Segmented eye image

(d) Normalized iris image

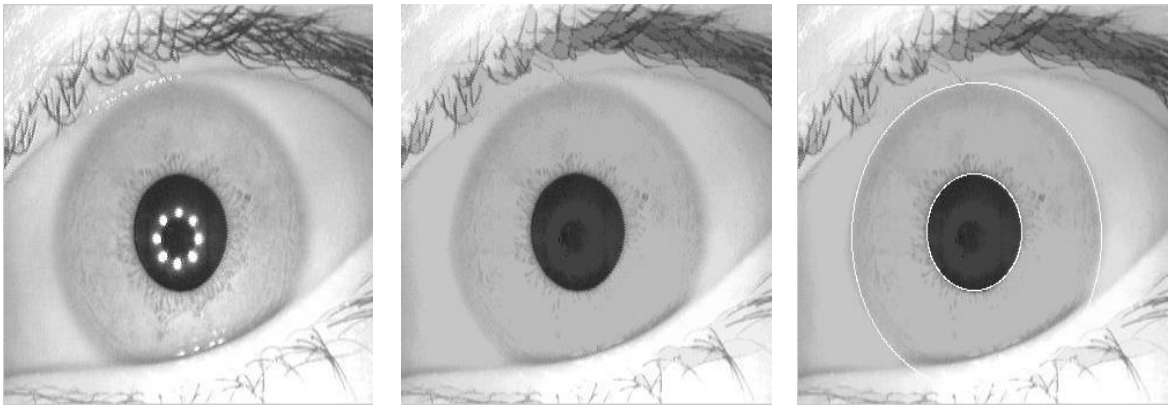

(e) Eye image of person-2 (f) Eye image with countered light reflections (g) Segmented eye image

(h) Normalized iris image

Figure 4.1: Experimental results of countered light reflections from eye images, segmented and normalized eye and iris images of four different persons from CASIA database.

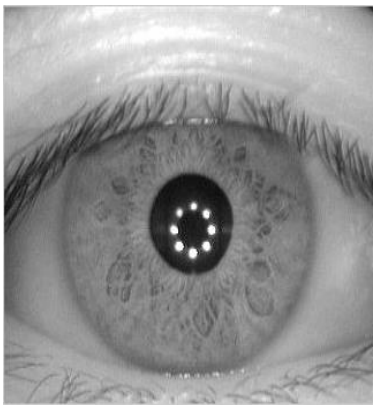

(i) Eye image of person-3

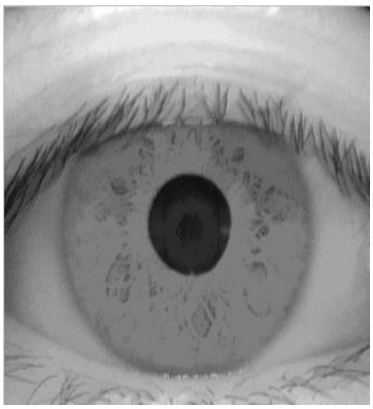

(j) Eye image with countered light reflections

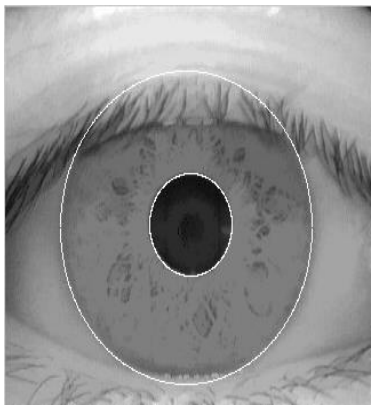

(k) Segmented eye image

(l) Normalized iris image

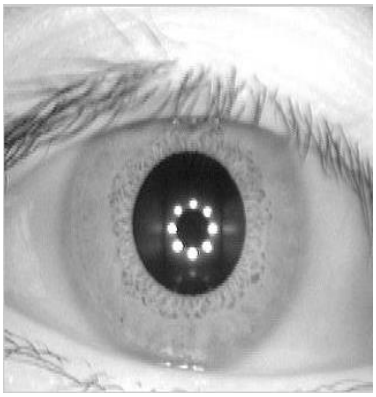

(m) Eye image of person-4

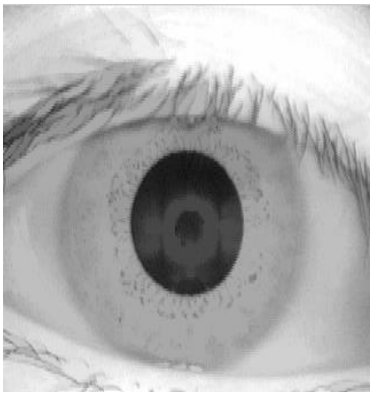

(n) Eye image with countered light reflections

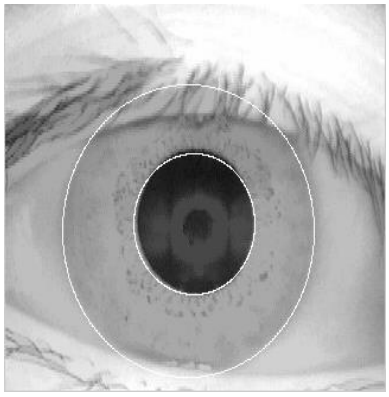

(o) Segmented eye image

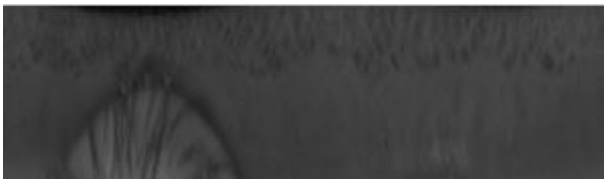

(p) Normalized iris image

Figure 4.1: Experimental results of countered light reflections from eye images, segmented and normalized eye and iris images of four different persons from CASIA database. (contd.)

4.3 EXPERIMENTAL OBSERVATIONS OF FEATURE VECTOR COEFFICIENT EXTRACTION BASED ON VARIOUS SCANNING TECHNIQUES

The coefficient feature extraction is the next step to follow after normalization of segmented iris. Extraction of FV coefficients is done on the basis of various scanning techniques after application of DCT on the normalized irises that create FV coefficient matrices. The observed results for 49 extracted FV coefficients based on various scanning techniques such as Zigzag, Raster Type-I Raster Type- II, Sawtooth Type-I, Sawtooth Type-II and Sawtooth Type-III scan for eye image of a person are illustrated in following subsection.

4.3.1 DISCRETE COSINE TRANSFORM APPLICATION ON AN EYE IMAGE

The step-wise illustration of DCT application over on eve image is shown in the Figure 4.2, 4.3, 4.4 and 4.5 respectively.

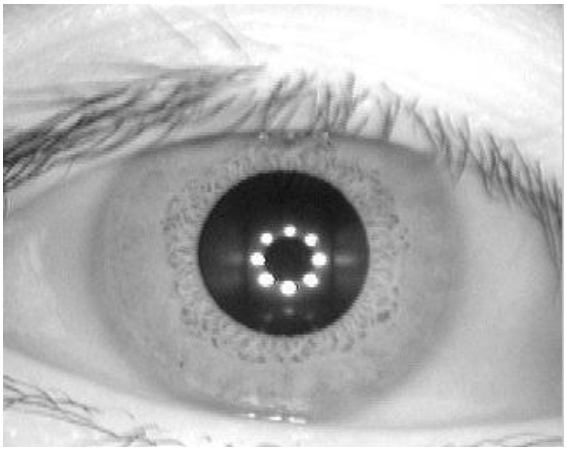

Figure 4.2: Eye image

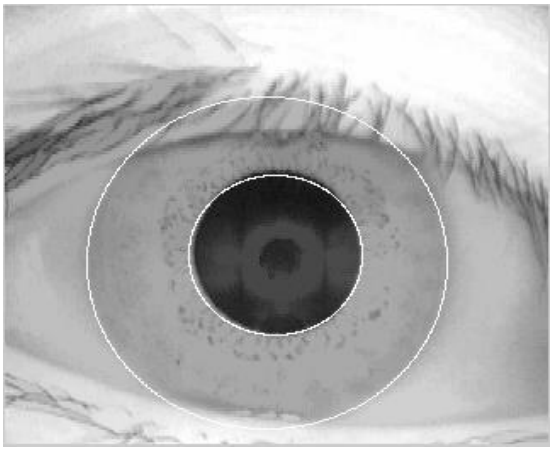

Figure 4.3: Segmented eye image

Figure 4.4: Normalized iris image

Figure 4.5: DCT application on normalized iris creating FV coefficient matrix

After the application of DCT, scanning methodologies are applied on the obtained matrix. Coefficient-wise scanning over the DCT applied matrix is shown in the following subsections.

4.3.1.1 ZIGZAG SCAN ON FV COEFFICIENT MATRIX

For feature extraction, when Zigzag scanning is applied, the pattern it follows is shown by the coefficient-wise scanning in the following matrix.

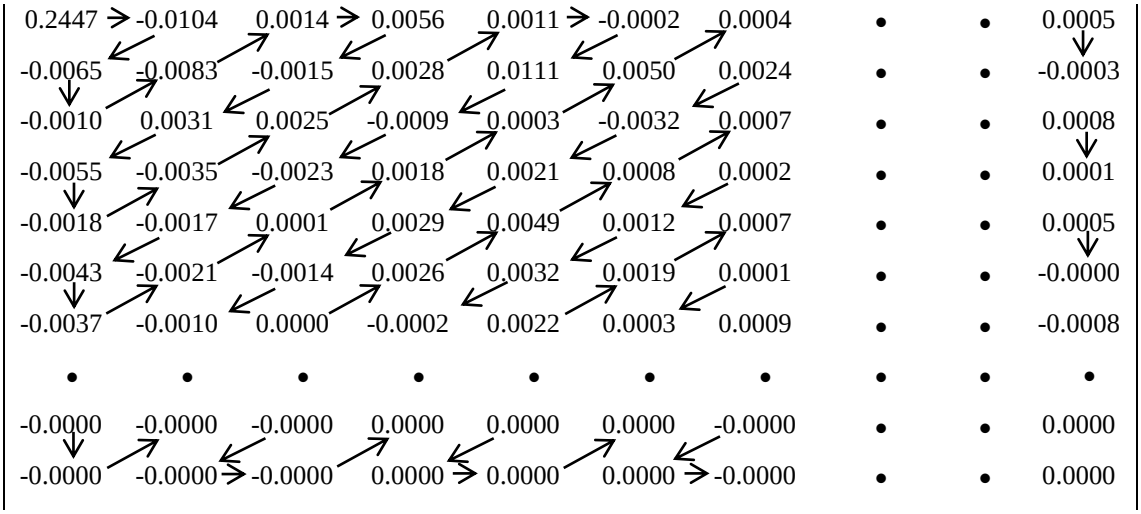

Implies, extracted 49 coefficients using Zigzag scan are,

[0.2447 -0.0104 -0.0065 -0.0010 -0.0083 0.0014 0.0056 -0.0015 0.0031
-0.0055 -0.0018 -0.0035 0.0025 0.0028 0.0011 -0.0002 0.0111 -0.0009
-0.0023 -0.0017 -0.0043 -0.0037 -0.0021 0.0001 0.0018 0.0003 0.0050
0.0004 0.0013 0.0024 -0.0032 0.0021 0.0029 -0.0014 -0.0010 -0.0039
-0.0028 -0.0014 0.0000 0.0026 0.0049 0.0008 0.0007 -0.0003 0.0015
0.0008 -0.0024 -0.0000 0.0002]

Figure 4.6: Illustration of extracted 49 coefficients using Zigzag scan

4.3.1.2 RASTER TYPE-I SCAN ON FV COEFFICIENT MATRIX

For feature extraction, when Raster Type-I scanning technique is applied, the pattern it follows is shown by the coefficient-wise scanning in the following matrix.

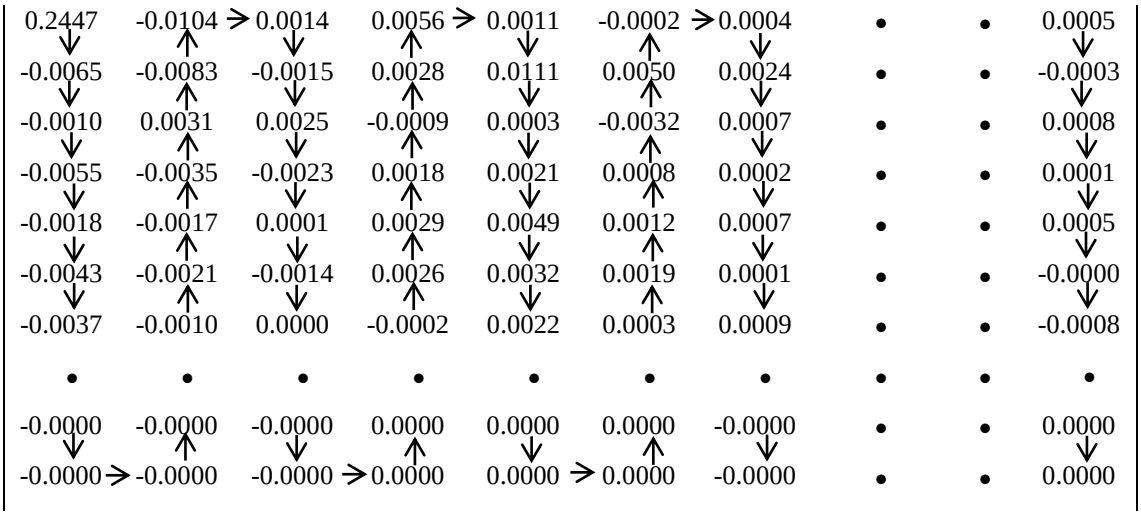

Implies, extracted 49 coefficients using Raster Type-I scan are,

[0.2447 -0.0065 -0.0010 -0.0055 -0.0018 -0.0043 -0.0037 -0.0039 -0.0028
-0.0017 -0.0015 -0.0017 -0.0016 -0.0017 -0.0007 -0.0008 -0.0007 -0.0010
-0.0008 -0.0007 -0.0007 -0.0004 -0.0005 -0.0004 -0.0003 -0.0003 -0.0003
-0.0001 -0.0001 -0.0002 -0.0002 -0.0001 -0.0002 -0.0002 -0.0002 -0.0001
-0.0000 -0.0001 -0.0001 -0.0001 -0.0002 -0.0001 -0.0001 -0.0001 -0.0001
-0.0001 -0.0001 -0.0001 -0.0001]

Figure 4.7: Illustration of extracted 49 coefficients using Raster Type-I scan

4.3.1.3 RASTER TYPE-II SCAN ON FV COEFFICIENT MATRIX

For feature extraction, when Raster Type-II scanning technique is applied, the pattern it follows is shown by the coefficient-wise scanning in the following matrix.

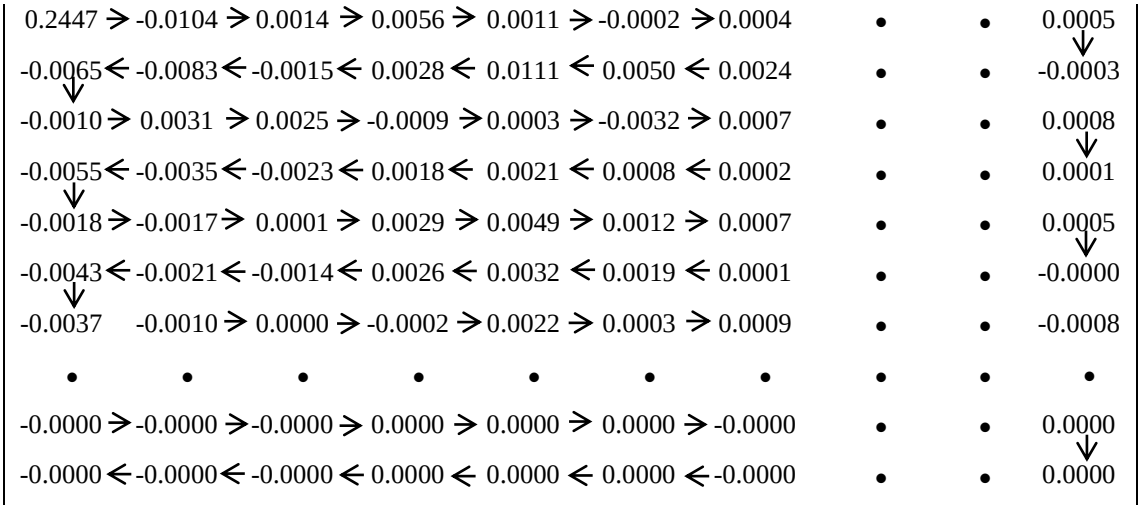

Implies, extracted 49 coefficients using Raster Type-II scan are,

[0.2447 -0.0104 0.0014 0.0056 0.0011 -0.0002 0.0004 0.0013 0.0015
0.0008 0.0012 0.0018 0.0014 0.0009 0.0012 0.0008 -0.0011 -0.0003
-0.0001 -0.0008 -0.0011 -0.0003 -0.0008 -0.0005 0.0001 -0.0001 -0.0003
0.0006 -0.0002 -0.0002 -0.0007 0.0001 -0.0001 0.0005 0.0013 0.0003
0.0001 -0.0003 -0.0015 -0.0004 -0.0016 -0.0007 0.0005 0.0004 0.0011
0.0008 0.0003 0.0004 0.0001]

Figure 4.8: Illustration of extracted 49 coefficients using Raster Type-II scan

4.3.1.4 SAWTOOTH TYPE-I SCAN ON FV COEFFICIENT MATRIX

For feature extraction, when Sawtooth Type-I scanning technique is applied, the pattern it follows is shown by the coefficient-wise scanning in the following matix.

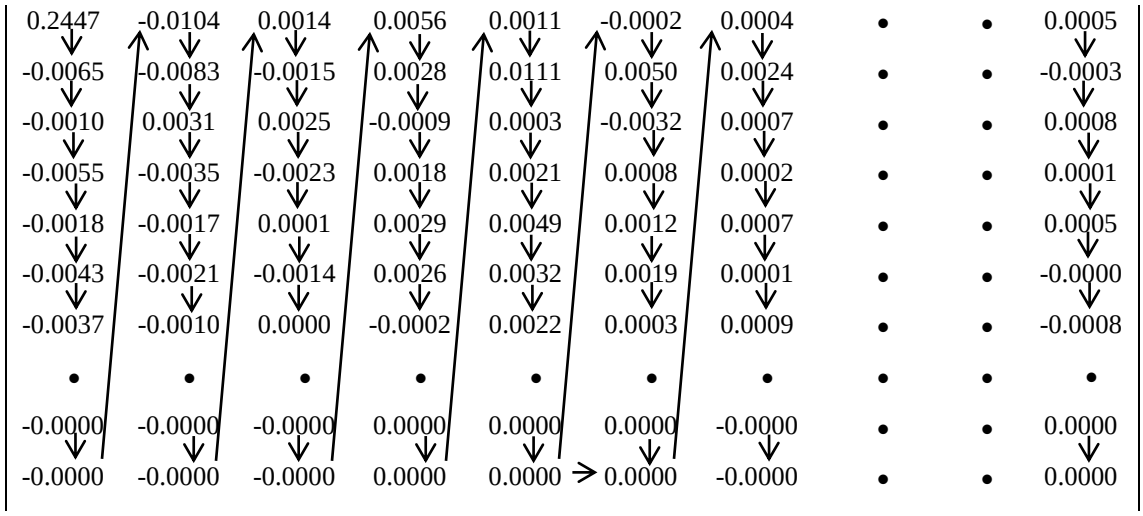

Implies, extracted 49 coefficients using Sawtooth Type-I scan are,

[0.2447 -0.0065 -0.0010 -0.0055 -0.0018 -0.0043 -0.0037 -0.0039 -0.0028
-0.0017 -0.0015 -0.0017 -0.0016 -0.0017 -0.0007 -0.0008 -0.0007 -0.0010
-0.0008 -0.0007 -0.0007 -0.0004 -0.0005 -0.0004 -0.0003 -0.0003 -0.0003
-0.0001 -0.0001 -0.0002 -0.0002 -0.0001 -0.0002 -0.0002 -0.0002 -0.0001
-0.0000 -0.0001 -0.0001 -0.0001 -0.0002 -0.0001 -0.0001 -0.0001 -0.0001
-0.0001 -0.0001 -0.0001 -0.0001]

Figure 4.9: Illustration of extracted 49 coefficients using Sawtooth Type-I scan

4.3.1.5 SAWTOOTH TYPE-II SCAN ON FV COEFFICIENT MATRIX

For feature extraction, when Sawtooth Type-II scanning technique is applied, the pattern it follows is shown by the coefficient-wise scanning in the following matix.

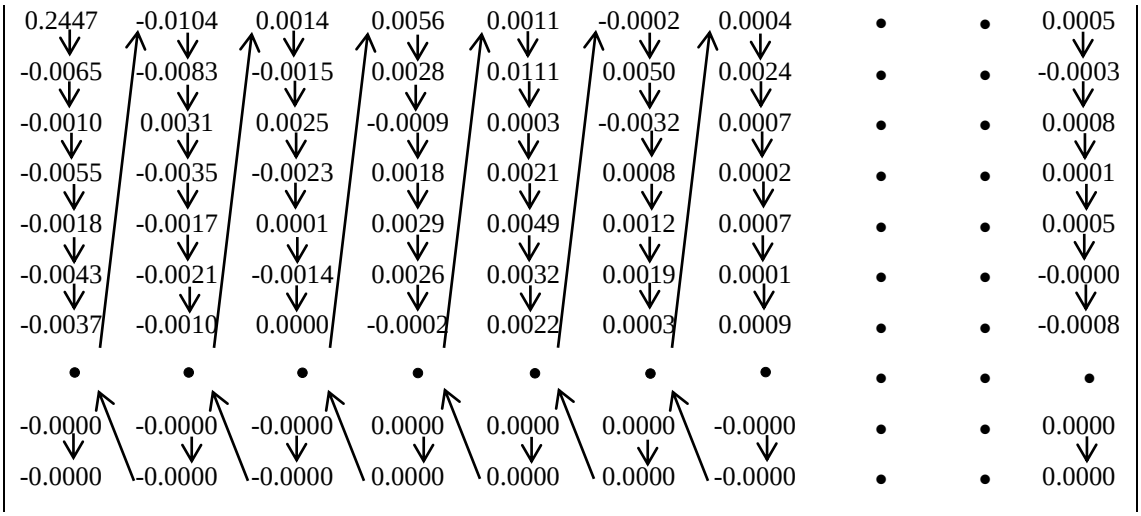

Implies, extracted 49 coefficients using Sawtooth Type-II scan are,

[0.2447 -0.0065 -0.0010 -0.0055 -0.0018 -0.0043 -0.0037 -0.0039 -0.0028
-0.0017 -0.0015 -0.0017 -0.0016 -0.0017 -0.0007 -0.0008 -0.0007 -0.0010
-0.0008 -0.0007 -0.0007 -0.0004 -0.0005 -0.0004 -0.0003 -0.0003 -0.0003
-0.0001 -0.0001 -0.0002 -0.0002 -0.0001 -0.0002 -0.0002 -0.0002 -0.0001
-0.0000 -0.0001 -0.0001 -0.0001 -0.0002 -0.0001 -0.0001 -0.0001 -0.0001
-0.0001 -0.0001 -0.0001 -0.0001]

Figure 4.10: Illustration of extracted 49 coefficients using Sawtooth Type-II scan

4.3.1.6 SAWTOOTH TYPE-III SCAN ON FV COEFFICIENT MATRIX

For feature extraction, when Sawtooth Type-III scanning technique is applied, the pattern it follows is shown by the coefficient-wise scanning in the following matrix.

Implies, extracted 49 coefficients using Sawtooth Type-III scan are,

[0.2447 -0.0065 -0.0104 -0.0083 0.0014 -0.0015 0.0056 0.0028 0.0011
0.0111 -0.0002 0.0050 0.0004 0.0024 0.0013 -0.0003 0.0015 -0.0024
0.0008 -0.0014 0.0012 -0.0011 0.0018 0.0005 0.0014 -0.0005 0.0009
-0.0018 0.0012 -0.0011 0.0008 0.0006 -0.0011 0.0001 -0.0003 0.0018

-0.0001 0.0005 -0.0008 0.0002 -0.0011 0.0002 -0.0003 -0.0003 -0.0008
-0.0004 -0.0005 -0.0000 0.0001]

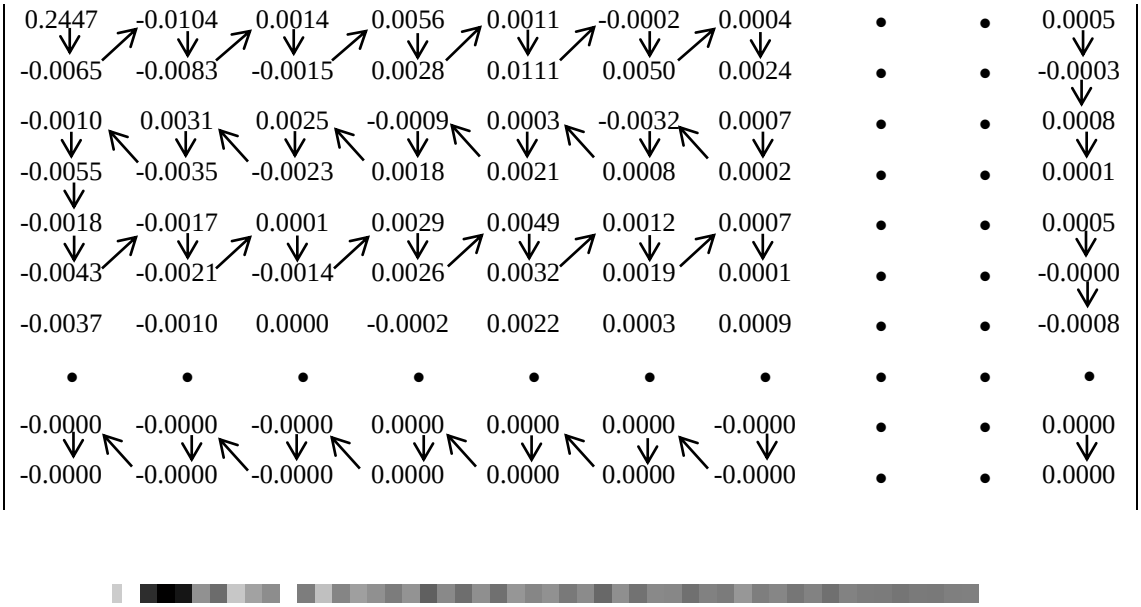

Figure 4.11: Illustration of extracted 49 coefficients using Sawtooth Type-III scan

4.3 ACURRACY ANALYSIS

FV coefficient extraction based on various scanning techniques after applying DCT over normalized iris image matrices is done so that matching using MSE is performed to analyze the accuracy. Accuracy percentage for partial FV coefficients is achieved by taking the ratio percentage of total number of individuals identified correctly to the total number of individuals.

$$Accuracy\ Percentage = \frac{Number\ of\ correctly\ identified\ individuals}{Total\ number\ of\ individuals} \times 100 \quad (4.1)$$

The accuracy results in the form of bar graph and percentage are compiled in Table 4.1 and Figure 4.3 respectively.

From the Table 4.1 it is observed that with different scanning techniques different accuracy percentages are attained. The best accuracy *i.e.* 80.30% is observed when 100 and 1024 coefficients are taken after Raster Type-II and Sawtooth Type-I scan respectively. But the best result is considered for the case when 100 FV coefficients are

taken after Raster Type-II scan being lesser than 1024 FV coefficients in case of Sawtooth Type-I scan. Also, taking only 148 coefficients *i.e.* only 1.48% coefficients of the FV matrix provides very good results for approximately all discussed scanning techniques. This may happen because of the property of DCT is energy concentration towards upper-left corner of 2-D matrix.

Table 4.1: Accuracy analysis for various coefficients from scanned FV matrix (in %age).

Sr. No.	**Number of FV Coefficients**	**Accuracy Percentage for Various Scanning Techniques**					
		Zigzag	**Raster Type-I**	**Raster Type-II**	**Sawtooth Type-I**	**Sawtooth Type-II**	**Sawtooth Type-III**
1	10000	62.12	62.12	62.12	62.12	62.12	62.12
2	9216	60.60	62.12	63.63	62.12	66.66	63.63
3	4096	66.66	63.63	60.60	63.63	60.60	63.63
4	2048	68.18	63.63	63.63	63.63	60.60	63.63
5	1536	68.18	72.72	62.12	68.18	62.12	62.12
6	1024	68.18	**78.78**	60.60	**80.30**	62.12	62.12
7	576	72.72	74.24	62.12	72.72	62.12	60.60
8	256	**78.78**	74.24	62.12	72.72	**74.24**	66.66
9	148	74.24	74.24	78.78	72.72	68.18	**78.78**
10	113	62.12	74.24	78.78	72.72	63.63	**78.78**
11	100	62.12	78.78	**80.30**	78.78	62.12	**78.78**
12	83	68.18	78.78	74.24	78.78	63.63	71.21
13	71	66.66	77.27	71.21	77.27	62.12	71.21
14	64	63.63	77.27	68.18	77.27	62.12	72.72
15	49	66.66	71.21	68.18	71.21	71.21	72.72
16	36	60.60	60.60	66.66	60.60	60.60	66.66
17	16	66.66	66.66	66.66	66.66	66.66	72.72
18	8	66.66	66.66	78.78	66.66	66.66	71.21
19	4	62.12	63.63	77.27	63.63	63.63	66.66
20	1	60.60	60.60	60.60	60.60	60.60	60.60

The bar graph shown in Figure 4.12 indicates the variation in accuracy percentage for different number of coefficients from FV matrix of individuals iris matrices for Zigzag, Raster Type-I, Raster Type-II, Sawtooth Type-I, Sawtooth Type-II and Sawtooth Type-III scan respectively on the basis of Table 4.1.

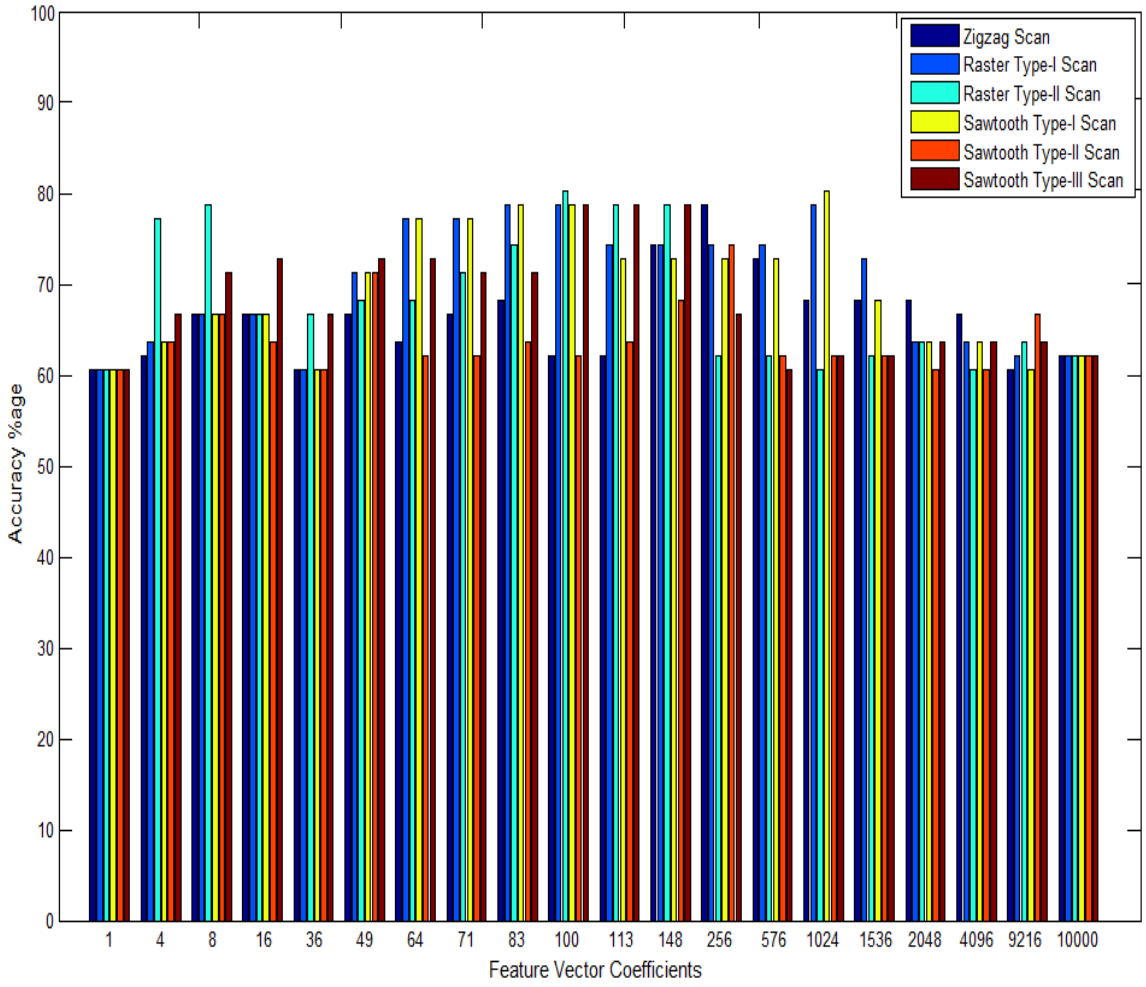

Figure 4.12: FV coefficients vs accuracy percentage bar chart

4.4 COMPARISON

The observed results of feature matching in the form of percentage as indicated in Table 4.1 are then compared with the related work proposed by Kekre *et al.* [51] which scans for FV matrix according to the Figure 2.7 shown in chapter 2. They calculated the results by reducing the FV matrix size from full image matrix size to 1×1 and obtained the best accuracy percentage of 79.68% at 7×7 FV matrix which is less than 80.30% accuracy results of proposed work. This may happen because the calculated results of related work are based on direct extraction of features from eye images rather than extracting iris region from the image of eye first and then rest of the processing is performed. Table 4.2 represents the comparison between the best accuracy percentage of the related and the

proposed work when 7×7 or 49 and 10×10 or 100 FV matrix and FV coefficients are extracted respectively. The Table 4.2 also indicates that the accuracy percentages of the introduced work is better than the related work but at the expense of increased computational complexity since more coefficients are required to give better results.

Table 4.2: Comparison between related (Kekre *et al*., [51]) and proposed work (in %age).

Feature Vector (FV) Matrix / Coefficients	**Accuracy Percentage for Various Scanning Techniques**						
	Kekre *et al.* [51]	**Proposed Work**					
	Matrix	**Zigzag**	**Raster Type-I**	**Raster Type-II**	**Sawtooth Type-I**	**Sawtooth Type-II**	**Sawtooth Type-III**
7×7 / 49	**79.6875**	66.66	71.21	68.18	71.21	71.21	72.72
10×10 / 100	78.1250	62.12	78.78	**80.30**	78.78	62.12	78.78

4.5 COMPLEXITY ANALYSIS

During matching of the scanned FV matrix, calculation of the MSE is the main task [51]. N subtractions are involved in calculation of difference between corresponding FV coefficients of two (1×N) matrices. Similarly, coefficients of difference matrix involve N number of multiplications. Thus, in order to compute the entire (1×N) answer matrix, N multiplications and N additions will be required. Since the CASIA database involves grey scaled images only, so the total number of required operations would be:

$$Total\ number\ of\ operations = N\ additions + N\ multiplications \quad (4.2)$$

The calculation of mean of the matrix (1×N) would involve N-1 additions and 1 division [51]. Consequently, the total number of operations required to calculate MSE would be:

$$Total\ number\ of\ operations = (2N - 1)\ additions + (N + 1)\ multiplications \quad (4.3)$$

Considering,

$$1\ addition\ operation = 1\ CPU\ unit \quad (4.4)$$

$$1\ multiplication\ operation = 8\ CPU\ unit \quad (4.5)$$

Hence, the required FV coefficients and CPU units are given in Table 4.3.

Thus, the complexity of the system has dropped dramatically which can be justified as only 0.010079% of the original CPU units are required number of CPU units.

Table 4.3: Total CPU units required for iris recognition.

Operations	**Total FV Coefficients (10000)**	**Optimized FV Coefficients (100)**
Total Additions	19999	199
Total Multiplications	10001	101
Total CPU Units	100008	1008

4.6 SUMMARY

In this chapter, observational results obtained after each step of processing such as segmentation, normalization and feature extraction with the help of images along with the final results of feature matching in the form of a table and bar graph indicating the performance accuracy of IRS are discussed. Comparison results between the related and the proposed work are also presented in a tabular form in this chapter. Also, calculations are done to analyze computational complexity of the system and the results showing lesser complexity for the performed processing of the system are presented by a table in this chapter.

CHAPTER

CONCLUSION AND FUTURE SCOPE

5.1 CONCLUSION

In the presented work, discussions on segmentation and normalization techniques used along with the feature extraction based on various introduced scanning techniques in the field of iris recognition is done. Here, DCT is applied on localized and normalized iris matrices and the resultant feature vector matrices are scanned using various scanning techniques. Partial feature vector coefficients are then taken upon the requirement after scanning to solve the purpose of iris recognition.

Maximum accuracy percentage *i.e.* 80.30% is achieved when 100 coefficients were extracted after Raster Type-II which is better than the related work but at the expense of increased computational complexity. Taking only 148 coefficients of the feature vector matrix provides very good results for approximately all discussed scanning techniques following the property of DCT. Thus by discarding 98.52% coefficients or by retaining only 1.48% coefficients, better performance and accuracy is achieved. Thus, attaining partial feature vector coefficients via scanning techniques provide good accuracy.

5.2 FUTURE SCOPE

- Since it is well known that in the signal processing, the Discrete Fractional Fourier Transform (DFrFT) shows much better results than DCT so it can be applied to iris for feature extraction purpose in place of DCT to have better results.
- Iridology is an alternative medical field where diseases can be detected by observing the change in iris patterns and textures based on the iridology chart prepared by the practitioners. Implies, the thesis work can be extended to detect various diseases such as diabetes, cancer, impaired organ *etc*.

REFERENCES

[1] A. Nait-Ali, "Hidden Biometrics: Towards Using Biosignals and Biomedical Images for Security Applications," *IEEE 7th International Workshop on Systems, Signal Processing and their Applications*, pp. 352-356, 2011.

[2] BSI Corporate, *http://shop.bsigroup.com/Browse-By-Subject/Biometrics/Why-use-biometrics/*, 2015.

[3] R. Duda, P. Hart, and D. Stork, *Pattern Classification*, Wiley Interscience, New York, 2001.

[4] S.A. Kautsar, S. Akbar, F.N. Azizah, "An Application Framework for Evaluating Methods in Biometrics Systems," *IEEE International Conf. on Data and Software Engineering*, pp.1-6, 2014.

[5] WhatIs Dictionary, *http://whatis.techtarget.com/search/query?q=Biometrics*, 2010.

[6] J.D. Woodward, C. Horn, J. Gatune and A. Thomas, *Biometrics: A Look at facial recognition*, Rand Corporation, Santa Monica, 2003.

[7] National Science and Technology Council, "Fingerprint Recognition," http://www.fbi.gov/about-*us/cjis/fingerprints_biometrics/biometric-center-of-excellence/files/fingerprint-recognition.pdf*, pp. 100-109, 2015.

[8] S.D. Fried, "Domain Access Control Systems and Methodology," *http://www.itu.dk/courses/SIAS/E2005/AU224001.pdf*, 2004.

[9] M.A.U. Bromba, "Biometrics FAQ's," *http://www.bromba.com/faq/biofaq.htm*. 2010.

[10] K. Fakhar, M. el Aroussi, M.N. Saidi, D. Aboutajdine, "Score Fusion in Multibiometric Identification based on Fuzzy Set Theory," *5th International Conf. on Image and Signal Processing*, vol. 7340, pp. 261-268, 2012.

[11] A.K. Jain, and A. Ross, "Multibiometric Systems," *Communications of ACM*. vol. 47, no. 1, pp. 34-40, 2004.

[12] S. Singh, and K. Singh, "Segmentation Techniques for Iris Recognition System," *International Journal of Scientific & Engineering Research*, vol. 2, no. 4, pp. 1-8, 2011.

[13] A.K. Jain, R. Bolle and S. Pankanti, *Biometris: Personal Identification in Networked Security*, 2nd ed., Kluwer Academic Publishers, E.U.A. 1999.

[14] "The History of Fingerprints," *http://onin.com/fp/fphistory.html*, 2015.

[15] S. Kaur, and G. Kaur, "Optimized Palm Recognition Using Cuckoo Search Algorithm," *International Journal of Advanced Research in Computer and Communication Engineering*, vol. 2, no. 11, pp. 4245-4250, 2013.

[16] Metrónomo, "Left Palm Print Taken Fingerprint Ink," *http://commons.wikimedia.org/wiki/File:Left_palm_print_-_1.svg*, 2013.

[17] A.K. Jain, B. Klare, U. Park, "Face Recognition: Some Challenges in Forensics," *IEEE International Conf. on Automatic Face and Gesture Recognition and Workshops*, pp. 726-733, 2011.

[18] D. Zhang and V. Kanhangad, "Hand Geometry Recognition," *Encyclopedia of Cryptography and Security*, pp. 529-531, 2011.

[19] R.S. Choras, "Hybrid Iris and Retina Recognition for Biometrics," *IEEE 3rd International Congress on Image and Signal Processing*, vol. 5, pp. 2422-2426, 2010.

[20] Göz Sagligi TV, "Retina Hakkında," *http://gozsagligi.tv/?p=66*, 2015.

[21] G.K.O. Michael, T. Connie, and A.B.J. Teoh, *Advanced Biometrics Technologies*, Croatia: INTECH, 2011.

[22] A.A. Ahmed, I. Traore, "Biometric Recognition based on Free-Text Keystroke

Dynamics," *IEEE Trans. on Cybernetics*, vol. 44, no. 4, pp. 458-472, 2014.

[23] A.K. Jain, A. Ross, and S. Prabhakar, "An Introduction to Biometric Recognition," *IEEE Trans. on Circuits and Systems for Video Technology*, vol. 14, no. 1, pp. 4-19, 2004.

[24] J.D. Woodward, K.W. Webb, E.M. Newton, M.A. Bradley, D. Rubenson, *et al*., *Army Biometric Applications – Identifying and Addressing Socio-Cultural Concerns*, Rand Corporation, Santa Monica, 2001.

[25] S. Liu, and M. Silverman, "A Practical Guide to Biometric Security and Technology," *IT Professional*, vol. 3, no. 1, pp. 27-32, 2001.

[26] Fujitsu Computer Products of America, "Palm Vein Pattern Authentication Technology," pp. 1-12, 2006.

[27] Scientific American, *http://www.scientificamerican.com/article/comparing-traits/*, 2008.

[28] Biometrics and the courts, *http://ctl.ncsc.dni.us/biomet%20web/BMIndex.html/*, 2010.

[29] D.B.L. Bong, R.N. Tingang, and A. Joseph, "Palm Print Verification System," *Proc. of the World Congress on Engineering*, vol. 1, pp. 1-4, 2010.

[30] Idesia's Biometric Technologies, "Biometric Comparison Table," *http://www.idesia-biometrics.com/technology/biometric_comparison_table.html*, 2010.

[31] O. Percy, A. Waqar, "Iris Localization using Daugman's Algorithm," BSc. Disserrtation, Blekinge Institute of Technology, School of Engineerng, Sweden, 2010.

[32] K.R. Nobel, "Iris Recognition," SFRAN: MorphoTrust USA, 2013.

[33] X. Meng, Y. Yin, G. Yang, and X. Xi, "Retinal Identification Based on an

Improved Circular Gabor Filter and Scale Invariant Feature Transform," *Sensors*, vol. 13, no. 7, pp. 9348-9266, 2013.

[34] Argus Global, "Classification of Biometrics for 1:1 Authentication," *http://www.argus-global.com/classification-biometrics-1-1-authentication/*, 2014.

[35] Wikipedia, *http://en.wikipedia.org/wiki/Human_eye*, 2015.

[36] T.H. Williamson, "Retina Surgery," *http://www.retinasurgery.co.uk/images/Anatomy%20Content.pdf*, 2013.

[37] R.P. Wildes, "Iris Recognition: An Emerging Biometric Technology," *Proc. of the IEEE*, vol. 85, no. 9, pp. 1348–1363, 1997.

[38] K. Schreiner, "Biometric: Prospects for Going the Distance," *IEEE Intelligent Systems and their Applications*, vol. 14, no. 6, pp. 2-7, 1999.

[39] D.M. Monro, S. Rakshit, and D. Zang, "DCT-Based Iris Recognition," *IEEE Trans. on Pattern Analysis and Machine Intelligence*, vol. 29, no. 4, pp. 586-595, 2007.

[40] H.V. Carter, "Anatomy of the Human Body," *http://commons.wikimedia.org/wiki/File:Gray878.png#/media/File:Gray878.png*, 1918.

[41] J.G. Daugman, "High Confidence Visual Recognition of Persons by a Test of Statistical Independence," *IEEE Trans. on Pattern Analysis and Machine Intelligence*, vol. 25, no. 11, pp. 1148–1161, 1993.

[42] J.K. Pillai, V.M. Patel, R. Chellappa, and N. K. Ratha, "Secure and Robust Iris Recognition Using Random Projections and Sparse Representations," *IEEE Trans. on Pattern Analysis and Machine Intelligence*. vol. 33, no. 9, pp. 1877-1893, 2011.

[43] N.A. Jraerr, "Iris Segmentation Analysis using Integro-differential operator and Hough Transform," *http://www.slideshare.net/abujraerr/iris-segmentation-*

analysis-using-integro-differential-operator-and-hough-transform-in-biometric-system, 2013.

[44] C. Li, C. Xu, C. Gui, and M.D. Fox, "Level Set Evolution without Re-initialization: A New Variational Formulation," *Proc. of the IEEE*, vol. 1, pp. 430-436, 2005.

[45] C. Jayachandra, and V. Reddy, "Iris Recognition Based on Pupil Using Canny Edge Detection and K-Means Algorithm," *International Journal of Engineering and Computer Science*, vol. 2, no. 1, pp. 221-225, 2013.

[46] S. Jayalakshmi, and M. Sundaresan, "A Study of Iris Segmentation Methods using Fuzzy C-Means and K-Means Clustering Algorithm," *International Journal of Computer Applications*, vol. 85, no. 11, pp. 1-5, 2014.

[47] S. Thainimit, L. Alexandre, and V.M.N. de Almeida, "Iris Surface Deformation and Normalization," *International Symposium on Communications and Information Technologies*, pp. 501-506, 2013.

[48] W.W. Boles and B. Boashash, "A Human Identification Technique using Images of Iris and Wavelet Transform," *IEEE Trans. on Signal Processing*, vol. 46, no. 4, pp. 1185-1188, 1998.

[49] A. Nichal, P. Jadhav, V. Nikam, and V. Hipparkar, "DCT Based Iris Feature Extraction and Recognition for Security System," *International Journal of Advanced Research in Computer and Communication Engineering*, vol. 3, no. 5, pp. 6490-6494, 2014.

[50] M.H. Abhiram, C. Sadhu, K. Manikantan and S. Ramachandran, "Novel DCT Based Feature Extraction for Enhanced Iris Recognition," *International Conf. on Communication, Information & Computing Technology*, pp. 1-6, 2012.

[51] H.B. Kekre, T.K. Sarode, P. Bhatia, S.N. Nayak and D. Nagpal, "Iris Recognition Using Partial Coefficients by Applying Discrete Cosine Transform, Haar Wavelet and DCT Wavelet Transform," *International Journal of Computer Applications*,

vol. 32, no. 6, pp. 39-43, 2011.

[52] A. Panganiban, N. Linsangan, and F. Caluyo, "Wavelet-Based Feature Extraction Algorithm for an Iris Recognition System," *Journal of Information Processing Systems*, vol. 7, no. 3, pp. 425-434, 2011.

[53] C.A. Oluwakemi, J.S. Sadiku, S.A. Kayode, and G.J. Rasheed, "Iris Feature Extraction for Personal Identification Using Fast Wavelet Transform (FWT)," *International Journal of Applied Information Systems*, vol. 6, no. 9, pp. 1-6, 2014.

[54] M.T. Khan, D. Arora, and S. Shukla, "Feature Extraction through Iris Images Using 1-D Gabor Filter on Different Iris Datasets," *Proc. of the IEEE*, pp. 445-450, 2013.

[55] P. Yao, J. Li, X. Ye, Z. Zhuang, B. Li, "Iris Recognition Algorithm using Modified Log-Gabor Filters," *IEEE 18th International Conf. on Pattern Recognition*, vol. 4, pp. 461-464, 2006.

[56] S. Nisar, M.A. Khan, and M. Usman, "Iris Recognition Using Mel-Fequency Cepstra Coefficient," *International Journal of Engineering Research*, vol. 3, no. 2, pp. 126-129, 2014.

[57] S. Bradley, "3 Design Layouts: Gutenberg Diagram, Z-Pattern And F-Pattern," *http://www.vanseodesign.com/web-design/3-design-layouts/*, 2011.

[58] G. Bhatnagar, and Q.M.J. Wu, "Selective Image Encryption Based on Pixels of Interest and Singular Value Decomposition," *Digital Signal Processing*, vol. 22, pp. 648-663, 2012.

[59] "CASIA Iris Database," *http://biometrics.idealtest.org/*, 2013.

[60] D. de Martin-Roche, C. Sanchez-Avila, and R. Sanchez-Reillo, "Iris Recognition for Biometric Identification Using Dyadic Wavelet Transform Zero-Crossing," *IEEE 35th International Camahan Conf. on Security Technology*, pp. 272-277, 2001.

LIST OF PUBLICATIONS

K. Kaur and K. Singh, Localization and Feature Extraction based on Various Scanning Techniques in Iris Recognition, Turkish Journal of Electrical Engineering & Computer Sciences – *Communicated*, 2015. *(SCI Indexed)*

Turnitin Originality Report

Th1 by Kanwarpreet Kaur

From asa (aa111)

- Processed on 2015年07月10日 11:05 IST
- ID: 554961614
- Word Count: 10554

Similarity Index
9%
Similarity by Source

Internet Sources:
7%
Publications:
6%
Student Papers:
0%

sources:

1 2% match (Internet from 28-Sep-2012)
http://www.ijser.org
/researchpaper%5CSegmentation_Techniques_for_Iris_Recognition_System.pdf

2 1% match (Internet from 23-Oct-2014)
http://www.di.ubi.pt/~hugomcp/doc/TesePhD_HugoMCP.pdf

3 < 1% match (Internet from 28-Sep-2011)